GEOPHYSICAL AND PALEOSEISMOLOGICAL INVESTIGATIONS OF THE MARIANNA EARTHQUAKE SOURCE IN EAST-CENTRAL, ARKANSAS

Final Technical Report

Research supported by the U.S. Geological Survey (USGS),
Department of the Interior, under award G22AP00335

Principal Investigator
Martitia Tuttle

Co-Principal Investigators
Haydar Al-Shukri and Hanan Mahdi

Other Contributors
Rauf Hussein, Taher Ameen, and Kathleen Tucker

M. Tuttle & Associates
P.O. Box 345
Georgetown, ME 04548
Tel: 207-371-2007
E-mail: mptuttle@earthlink.net
URL: http://www.mptuttle.com

Project Period: 8/1/2022-2/28/2025

Program Element I: National & Regional Earthquake Hazards Assessments

Key Words: Paleoliquefaction, Paleoseismology, Age Dating

GEOPHYSICAL AND PALEOSEISMOLOGICAL INVESTIGATIONS OF THE MARIANNA EARTHQUAKE SOURCE IN EAST-CENTRAL, ARKANSAS

Principal Investigator
Martitia Tuttle

Co-Principal Investigators
Haydar Al-Shukri and Hanan Mahdi

Other Contributors
Rauf Hussein, Taher Ameen and Kathleen Tucker

M. Tuttle & Associates
P.O. Box 345
Georgetown, ME 04548

Abstract

On the basis of investigations of large, weathered sand blows and related sand dikes, the Marianna area at the southwestern end of the Reelfoot Rift has been recognized as a source of repeated, large, moment magnitude, **M**, > 6 earthquakes during the Middle-Early Holocene, and possibly the Late Pleistocene. The sand blows occur along a northwest-oriented tonal lineament, named the Daytona Beach lineament (DBL), beneath which a fault zone was interpreted from seismic reflection profiles. Previous investigations of sand blows along the DBL attributed them to three earthquakes between 4.5-10.2 thousand years ago (ka) and at least two earlier events between 11-41 ka, possibly resulting from slip events on the underlying fault zone.

During this project, investigations were conducted at three liquefaction sites – DBNW5, DBNW7, and DBNW8 – located towards the northern end of the DBL west of Marianna. Results of radiocarbon and optically-stimulated luminescence dating are used to estimate the ages of the large, weathered sand blows at the three sites. The liquefaction features are interpreted to have formed about 5.4 ka, probably during the same earthquake. This is likely the event previously estimated to have occurred 5.5 ka. The additional investigation of sand blows in the area has led to a reduction in the uncertainty in the age estimate of the event. Also, during this project, the results of previous investigations at sites DBSE2, DBNW2, and DBNW3 were reviewed and the age estimates of the liquefaction features, and thus the earthquakes that caused them, revised to 4.7 ka, 9.8 ka, and 15 ka and 24.3 ka, respectively.

Important lessons have been learned about dating large, weathered sand blows. Samples collected from the upper portions of buried soils provide relatively close maximum constraining ages for the overlying sand blows and thus the approximate timing of the earthquake(s) that led to their formation. The deeper the pre-event surface soils are buried by sand blows, the more likely organic material is preserved in the buried soils and the less likely the buried soils are disturbed by post-event bioturbation.

The sand at site DBNW2 was mined for construction purposes, completely destroying the sand blows and dikes that formed during the Late Pleistocene. Other liquefaction sites have been leveled, sometimes by 1+ m, for agricultural purposes. Time is of the essence for recovering the record of paleoearthquakes in the Marianna area and surrounding region before it is lost forever.

Introduction

Paleoliquefaction studies provide information about the timing, location, magnitude, and recurrence times of large paleoearthquakes (e.g., Obermeier, 1996; Tuttle, 2001; Tuttle et al., 2019a,b). This type of information is crucial for assessing earthquake hazard in regions such as the Central and Eastern United States where active faults rarely rupture the ground surface or are otherwise difficult to recognize. On the basis of several paleoliquefaction studies (Al-Shukri et al., 2005, 2006, 2009, 2015; Tuttle et al., 2006, 2020; Tuttle and Hartleb, 2012), the Marianna area, located about 80 km south of the southern end of the New Madrid seismic zone (NMSZ) and 70 km southwest of Memphis, TN, has been recognized as a source of repeated large-magnitude earthquakes between about 5-10 ka and possibly earlier (Figures 1 and 2). As a consequence, the Marianna source was included in the Central and Eastern U.S. Seismic Source Characterization project (CEUS SSCP; Technical Report, 2012), the 2014 National Probabilistic Seismic Hazard Maps (Petersen et al., 2014), and most recently, the 2023 National Seismic Hazard Model (Thompson Jobe et al., 2022; Petersen et al., 2024).

In the Marianna area, where only a few small earthquakes have been recorded during the instrumental period, very large sand blows were found west and southwest of the town of Marianna in the Western Lowlands and northeast of Marianna in the St. Francis Basin (Figures 1 and 2; Al-Shukri et al., 2005, 2006; Tuttle et al., 2006). Most of the sand blows have deeply weathered profiles suggesting that they are thousands of years old. Of all the sand blows that have been dated so far, none formed less than 4.5 ka or are similar in age to known paleoearthquakes produced by the New Madrid seismic zone.

In the Western Lowlands, large sand blows are concentrated along, but not limited to, a northwest-oriented tonal lineament, referred to as the Daytona Beach lineament (DBL). Dating at multiple sites suggested that the sand blows formed during three earthquakes between 4.5-10.2 ka and two earthquakes between 11-41 ka (Figure 2). At two of the liquefaction sites (DBSE2 and DBNW2) along the DBL, soft-sediment faults were observed crosscutting sand dikes and soil lamellae that had developed in the dikes. The soft-sediment faults are parallel to the DBL as well as the feeder dikes, suggesting that emplacement of the sand dikes was fault-controlled (Tuttle et al., 2006; Al-Shukri et al., 2015).

To determine whether or not the DBL and associated sand blows might be related to faulting at depth, seismic reflection data was collected along two transects that crossed the DBL in the vicinity of DB1, Nancy2, and DBSE2 (Figure 2). The seismic-reflection profiles revealed a zone of near-vertical faults in the 100-1100-meter depth range, which likely includes Eocene through Paleozoic strata (Odum et al., 2016). The fault zone occurs beneath the DBL and associated sand blows. The seismic reflection study also found that fault displacements increase with depth, suggesting long-term recurrent faulting. These findings support the interpretation that the DBL and the associated sand blows are the surface expression of a fault zone that repeatedly produced large earthquakes (Tuttle et al., 2006, 2020; Al-Shukri et al., 2009, 2015).

In the St. Francis Basin, a compound sand blow and related sand dikes (SF500) were found buried beneath backswamp deposits in a cutbank exposure of the St. Francis drainage ditch (Figure 2; Tuttle et al., 2006). Dating at the site suggests that the liquefaction features formed circa 6.8 ka. The compound sand blow, composed of 6 depositional units, likely formed as the result of a sequence of large earthquakes, similar to the compound sand blows that formed as the result of the 1811-1812 New Madrid earthquakes (Tuttle et al., 2019a). The compound sand blow at SF500 occurs near the intersection of the Eastern Reelfoot Rift Margin fault zone

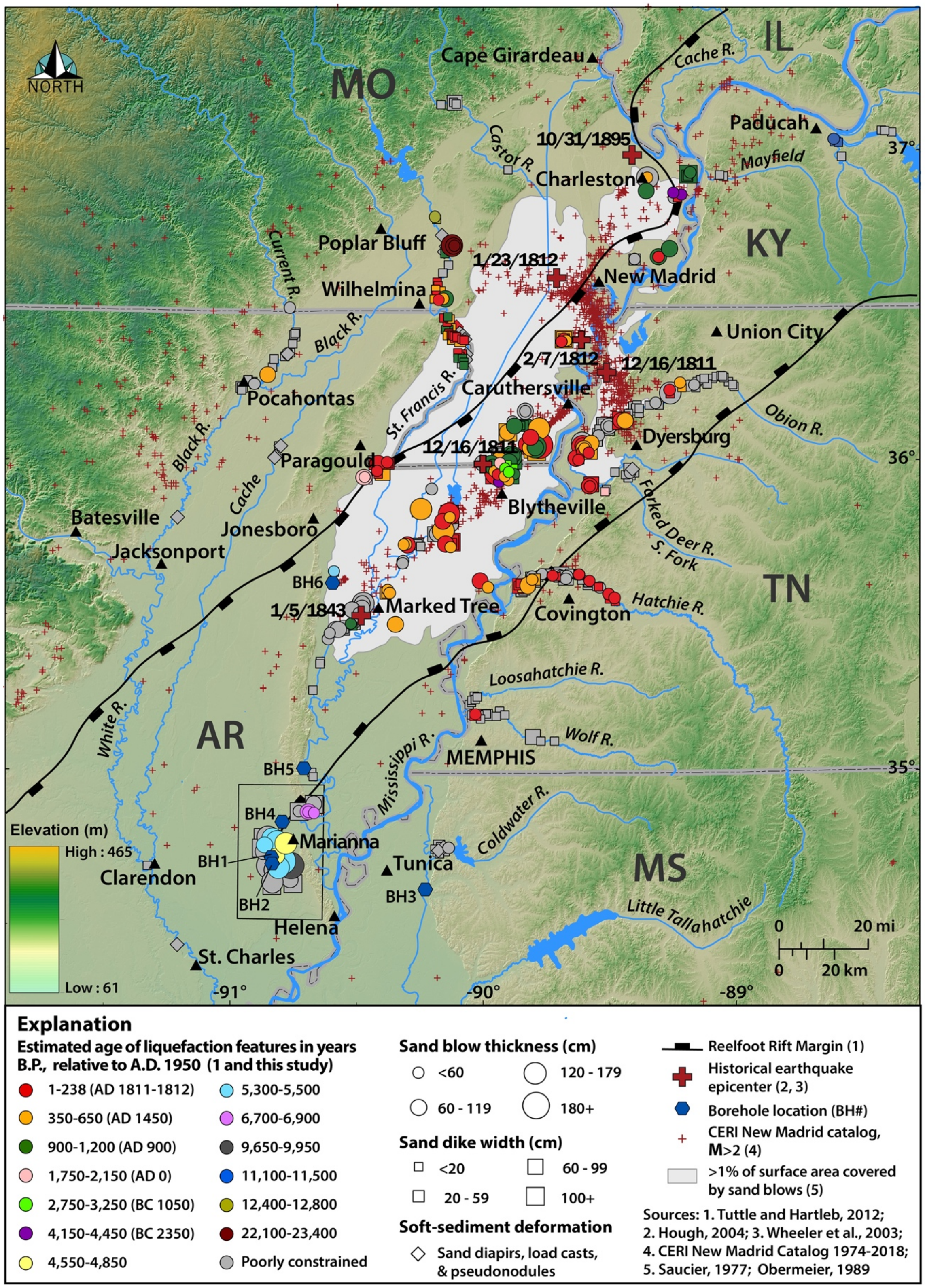

Figure 1. Shaded relief map of the Marianna area (outlined by black rectangle) and the New Madrid seismic zone (NMSZ; delineated by seismicity), showing locations, measured sizes, and estimated ages of earthquake-induced liquefaction features. The Marianna area is located near the southern end of the eastern Reelfoot Rift margin.

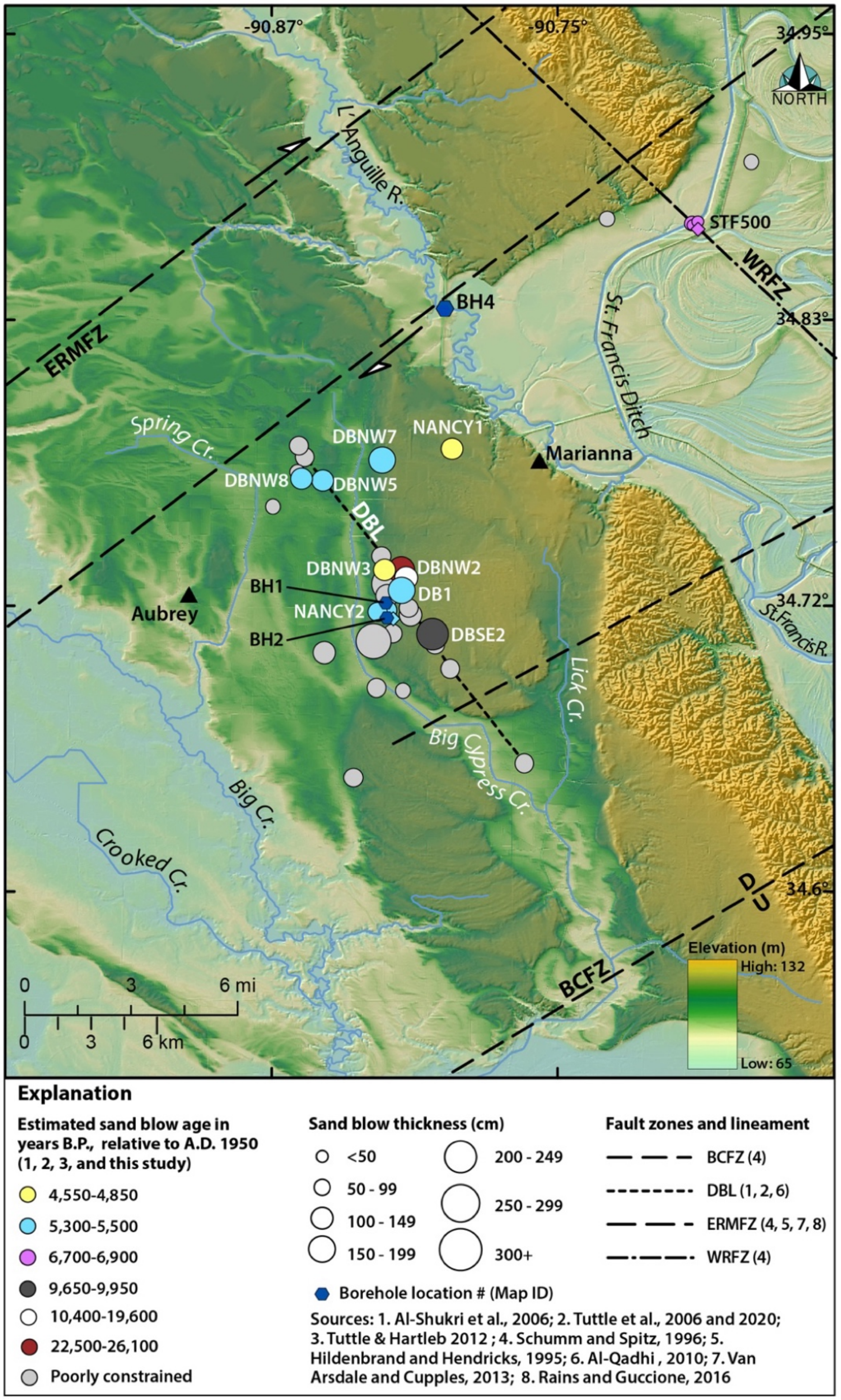

Figure 2. Shaded relief map of the Marianna area (delineated on Figure 1 with black rectangle), showing the Daytona Beach lineament (DBL) as well as locations, measured sizes, and estimated ages of sand blows studied during this and previous NEHRP grants. During this study, investigations were conducted at sites DBNW5, DBNW7, and DBNW8, and results of previous investigations were reviewed for sites DBSE2, DBNW2, and DBNW3.

(ERMFZ) and the White River fault zone (WRFZ). Exactly which faults were responsible for the earthquakes is not yet known, but might include the ERMFZ, the WRFZ, and possibly the fault zone beneath the DBL.

Liquefaction potential analysis (e.g., Seed and Idriss, 1971, 1982; Youd et al., 2001; Youd and Idriss, 2003; Juang and Jiang, 2000; Robertson, 2010; Juang et al., 2017) suggested that earthquakes of **M** 6-6.5 produced by the fault zone beneath the DBL could account for liquefaction at the sites in the Marianna area (Al-Shukri et al., 2015). However, relatively small liquefaction features found northwest of Blytheville and Marked Tree, Arkansas, and east of Tunica, Mississippi, are similar in age to three of the Marianna earthquakes (4.7 ka, 5.4 ka, and 6.8 ka events) and may represent distal effects of the Marianna events (Tuttle et al., 2019b). Further analysis indicates that larger Marianna earthquakes would be required to induce liquefaction at the distal sites. A Marianna earthquake in the **M** 7.2-7.5 range could account for a small sand blow northwest of Blytheville, Arkansas, and sand dikes along Coldwater River east of Tunica, Mississippi, that are similar in age to the 4.8 ka event; a Marianna earthquake in the **M** 6.9-7.5 range could account for a small sand blow and related dikes near Ditch 10 northwest of Marked Tree, Arkansas, that are similar in age to the 5.5 ka event; and a Marianna earthquake in the **M** 6.3-7.0 range could explain a small sand blow and sand dikes along the Coldwater River east of Tunica, Mississippi, that are similar in age to the 6.8 ka event (Tuttle et al., 2020).

The purpose of this study was to gain additional understanding of the paleoearthquakes produced by the Marianna source, especially those during the Late Pleistocene, by conducting additional site investigations of sand blows and related dikes. Our efforts were somewhat stymied by the destruction of Late Pleistocene sand blows at site DBNW2. As presented below, the site investigations at three new sites towards the northern end of the DBL, as well as review of the results of three prior site investigations, have improved age estimates of Marianna paleoearthquakes. In addition, important lessons have been learned about dating old, weathered sand blows which will contribute to future paleoliquefaction studies.

Site Investigations

GPR surveys and trench investigations were conducted at DBNW5, DBNW7, and DBNW8 during the late summer and fall of 2023. For methodology and equipment used in the GPR surveys, please see Chlaib et.al (2014) and Hussein, et.al. (2023). Based on the GPR surveys, we sited trenches so they crossed the main feeder dikes of the sand blows at the sites. Following the harvest of crops in October, we excavated the trenches to study the liquefaction features. We reopened the western portion of the southern trench at DBNW5, excavated a 45-m-long trench at DBNW7, and a 16-m-long trench at DBNW8. Because the summer and fall were exceptionally hot and dry, the soil and sediment exposed in the trenches were dry and crumbly, making it difficult to clean the trench walls. We sprayed the walls with water and scraped them as best we could. We examined both walls and the floors of the trenches for sand dikes and logged the portions of the trenches where the vent areas of the main feeder dikes and sand blows were exposed. We scoured the trench walls, especially the buried soils below the sand blows, for organic samples and collected samples for radiocarbon dating. We also collected sediment samples of the sand blow, buried soil, and subsoil for OSL dating. We revisited DBNW2 with the intention of collecting and dating samples to improve the age estimates of large sand blows and dikes that formed during the Late Pleistocene. Unfortunately, the entire site had been excavated and the sand removed for construction purposes. During this project, we also reviewed data previously collected at DBSE2, DBNW2, and DBNW3, and based on that review, revised the age estimates of large sand blows and related sand dikes at those sites. Summaries of the new investigations at DBNW5, DBNW7, and DBNW8, as well as the previous investigations at DBSE2, DBNW2, and DBNW3, are presented below. Calibrated ^{14}C and OSL ages at 1-standard deviation used to estimate the time of formation of sand blows and related dikes are provided in Tables 1-5 following the summaries. Although both ^{14}C and OSL ages are considered in estimating the age and liquefaction features, ^{14}C ages are often given preference due to their stratigraphic positions and/or smaller error ranges.

Daytona Beach Northwest 5 Site (DBNW5)

GPS Location:

South trench: 34.7679°N, 90.8461°W

North trench: Collapsed due to flooding during two tropical storms

Observations from GE satellite image and geophysical profiles (Figures 3-4):

Width of Sand Blow: 36 m from GPR survey

Length of Sand Blow: 64 m from GPR survey

Observations from South trench (Figure 5):

Thickness of Sand Blow: 1.4 m including plow zone

Width of Sand Dike: 2.7 m measured perpendicular to strike of the dike

Weathering Characteristics: Sand blow is very weathered; iron staining and formation of small to medium Fe-Mn nodules in upper 40 cm and large nodules above basal contact with buried soil.

Other Notable Features: The buried soil is displaced downward ~1.1 m on the northeast side of the dike. Large clasts of clayey silt occur in the sand blow above large sand dike.

Constraining Ages of Sand Blow from South trench (Figure 5; Tables 1, 4, and 5):

^{14}C dating of organic-rich sediment samples SL1 and SL2 from the top of the buried soil on either side of the large dike provide fairly close maximum constraining ages of 5,474-5,577 yr B.P. and 5,327-5,476 yr B.P., respectively. Giving preference to the younger ^{14}C age, the sand blow formed about 5.4 ka.

OSL dating of sample OSL 3 from the top of the buried soil provides a close maximum constraining age of 5,110 ± 120 yr B.P. and OSL 4 from 16 cm below the top of the buried soil provides a maximum constraining age of 7,475 ± 235 yr B.P. The OSL age of sample OSL 3 is in fairly close agreement with the ^{14}C ages of SL1 and SL2. The OSL age of sample OSL 4 is consistent with the younger age of OSL3 collected higher in the buried soil. OSL3 and OSL4 are more deeply buried and have lower dispersion values than OSL1 and OSL 2 suggesting that they are less likely to be mixed (Tables 4 and 5).

Age Estimate: 5.4 ka (range 5,327-5,476); preference given to maximum constraining age from ^{14}C dating.

Reference: Tuttle M. P., Al-Shukri, H, and Mahdi, H., 2020, Geophysical and paleoseismic investigations of large sand blows along a northwest-oriented lineament near Marianna, Arkansas, Final Technical Report, U.S. Geological Survey award G18AP00083, 31 p.

Figure 3. Google Earth satellite image acquired June 2016 showing a very large sand blow (light-colored soils) at site DBNW5, locations of GPR profiles 43, 44, 45, 46, and 47 (yellow lines), and locations of two paleoseismic trenches (heavy black lines).

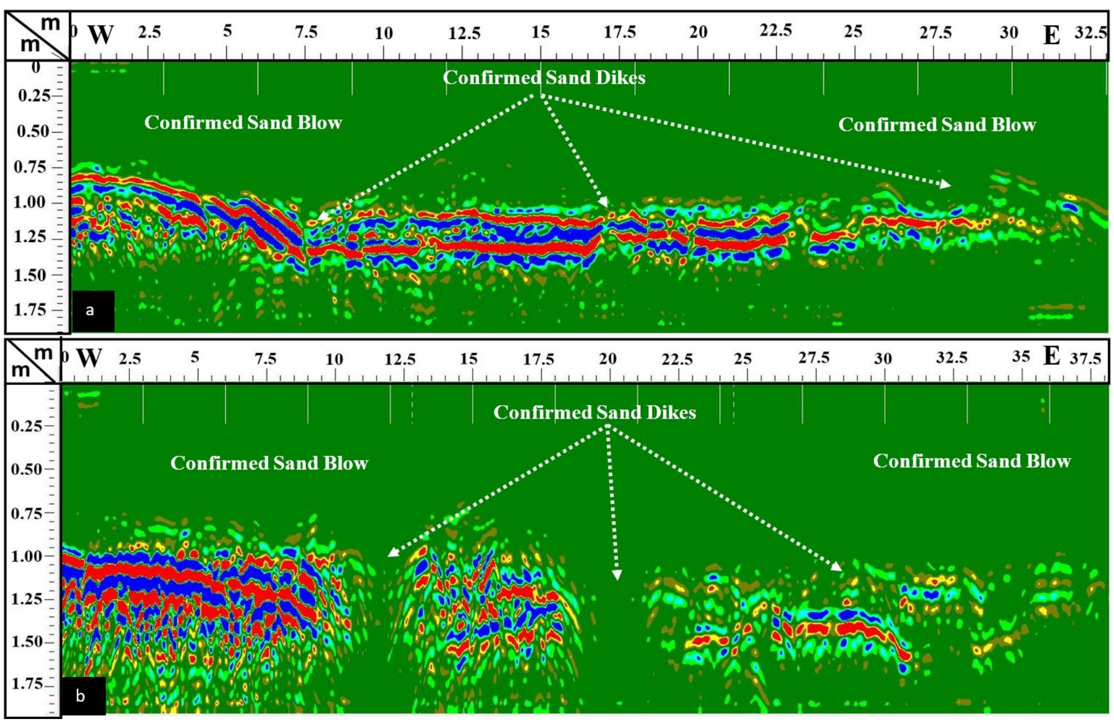

Figure 4. GPR profiles 44 (upper) and 43 (lower) show deformation of a strong reflector (red and blue bands) which represents the contact between the sand blow above and buried silty soil below. Discontinuities in the contact are related to ground failure and sand dikes.

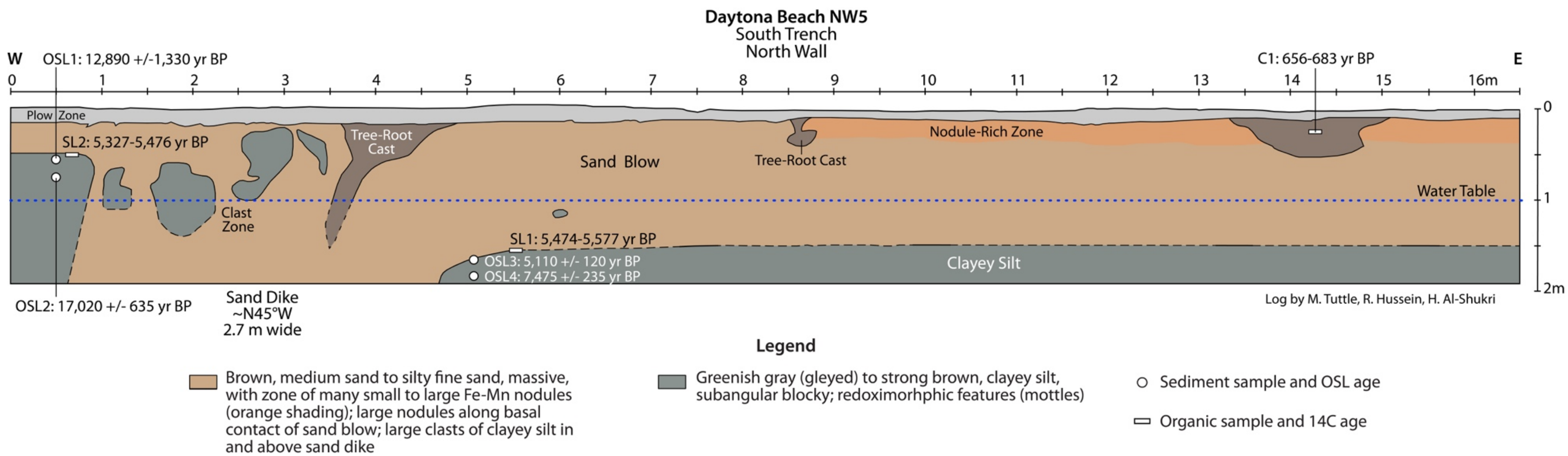

Figure 5. Log of the north wall of the southern trench excavated in the sand blow at site DBNW5. The trench was excavated along the transect of GPR profile 43 (see Figures 3 and 4) and shows a cross section of the large sand blow, large sand dike, and buried soil, as well as the positions of ^{14}C and OSL samples. Large clasts of the silty clay soil were concentrated in the sand blow above the large sand dike. The sand blow was very weathered and included a zone of small Fe-Mn nodules in the upper part of the sand blow and also large nodules towards the bottom of the sand blow. It rained during logging of the sand blow and the trenches filled with water and partially collapsed. Following the storm, the high-water table (dotted blue line) and buttressed trench walls made it difficult to log the contact between the sand blow and underlying soil (dashed where inferred). The site was revisited in 2023 and additional samples collected for dating. ^{14}C and OSL dating of the buried soil adjacent to the dike provides fairly close maximum constraining ages for the liquefaction features and indicate that they formed during an event about 5.4 ka.

Daytona Beach Northwest 7 Site (DBNW7)

GPS Location of trench: 34.7761°N, 90.8216°W

Observations from GE satellite image and geophysical profiles (Figures 6 and 7):

Width of Sand Blow: 45 m from GPR survey

Length of Sand Blow: 60 m from GPR survey

Observations from trench (Figure 8):

Thickness of Sand Blow: 1.5 m including plow zone

Width of Sand Dike: 49 cm

Weathering Characteristics: Sand blow is very weathered with redoximorphic features throughout and few areas of intense iron staining with small Fe-Mn nodules.

Other Notable Features: Few clasts of clayey silt in sand blow. Vent structure above the dike crosscuts the sand blow and is filled with silty, very fine sand (final phase of venting). The buried soil is displaced downward about 0.5 m on the east side of the dike.

Constraining Ages of Sand Blow from trench (Figure 8; Tables 1 and 5):

^{14}C dating of sample C2 of charred material collected near the tip of a root cast that extended through the sand blow and into the buried soil provides a minimum constraining age of 1,179 yr B.P. The contact of the buried soil was bioturbated, especially on the west side of the dikes, making it difficult to sample an undisturbed portion of the buried soil.

OSL2 collected from the upper 5 cm of the buried soil yielded an age of 41,445 ± 2,060 yr B.P. In addition to the large uncertainty in the age, the sample had a high dispersion value, suggesting that it was mixed with the older sand of the overlying sand blow. Therefore, the OSL age may more closely reflect the age of the vented sand than the age of the buried soil.

OSL 3 collected 15 cm below the top of the buried soil, where bioturbation was less severe, yielded an age of 7,200 ± 180 yr B.P. Its uncertainty range was relatively small and dispersion value low, lending confidence in the age. Given the similarity in the age of OSL 3 with that of OSL 4 (7,475 ± 235 yr B.P.) collected 16 cm below the top of the buried soil at site DBNW5, the sand blow and dike at DBNW7 are interpreted to have formed at same time as the liquefaction features at DBNW5 or about 5.4 ka.

OSL1 and OSL4 were collected from the upper portion of the sand blow and yielded ages of 16,285 ± 1,395 yr B.P. and 17,205 ± 1,350 yr B.P., respectively. The ages of both samples had large uncertainties and OSL1 had a high dispersion value of 44 ± 4, suggesting that it was either mixed or only partially bleached. Assuming the sand blow did form about 5.4 ka, the ages of OSL1 and OSL4 from the upper part of the sand blow are much too old. This suggests that the sand vented from below to the ground surface as the result of earthquake-induced liquefaction was only partially bleached, or in other words, grain luminescence was only partial reset by the sun. This could be due to rapid deposition of the sand during venting.

Age Estimate: 5.4 ka (range 5,327-5,476); based on dating at DBNW7 and nearby DBNW5)

Figure 6. Google Earth satellite image acquired June 2016 of site DBNW7 showing a very large sand blow (light-colored soils), locations of ground-penetrating radar (GPR) profiles 151-158 (yellow lines), and locations of one paleoseismic trench (heavy black line).

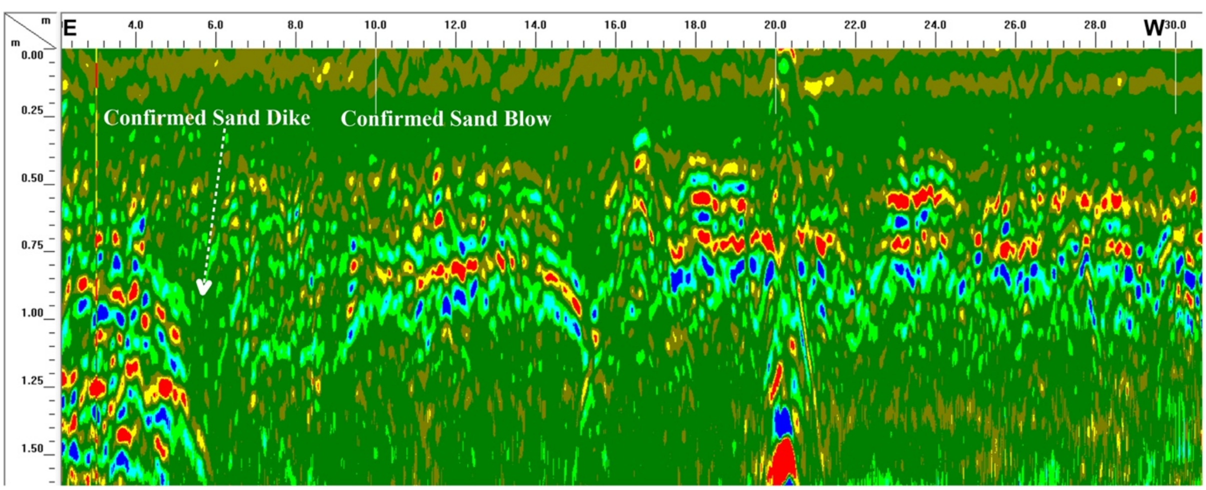

Figure 7. GPR profile 156 shows deformation of a strong reflector (red and blue bands) which represents the contact between the sand blow above and buried silty soil below. A sand blow and related sand dike (identified towards east end of the profile) were confirmed in the paleoseismic trench.

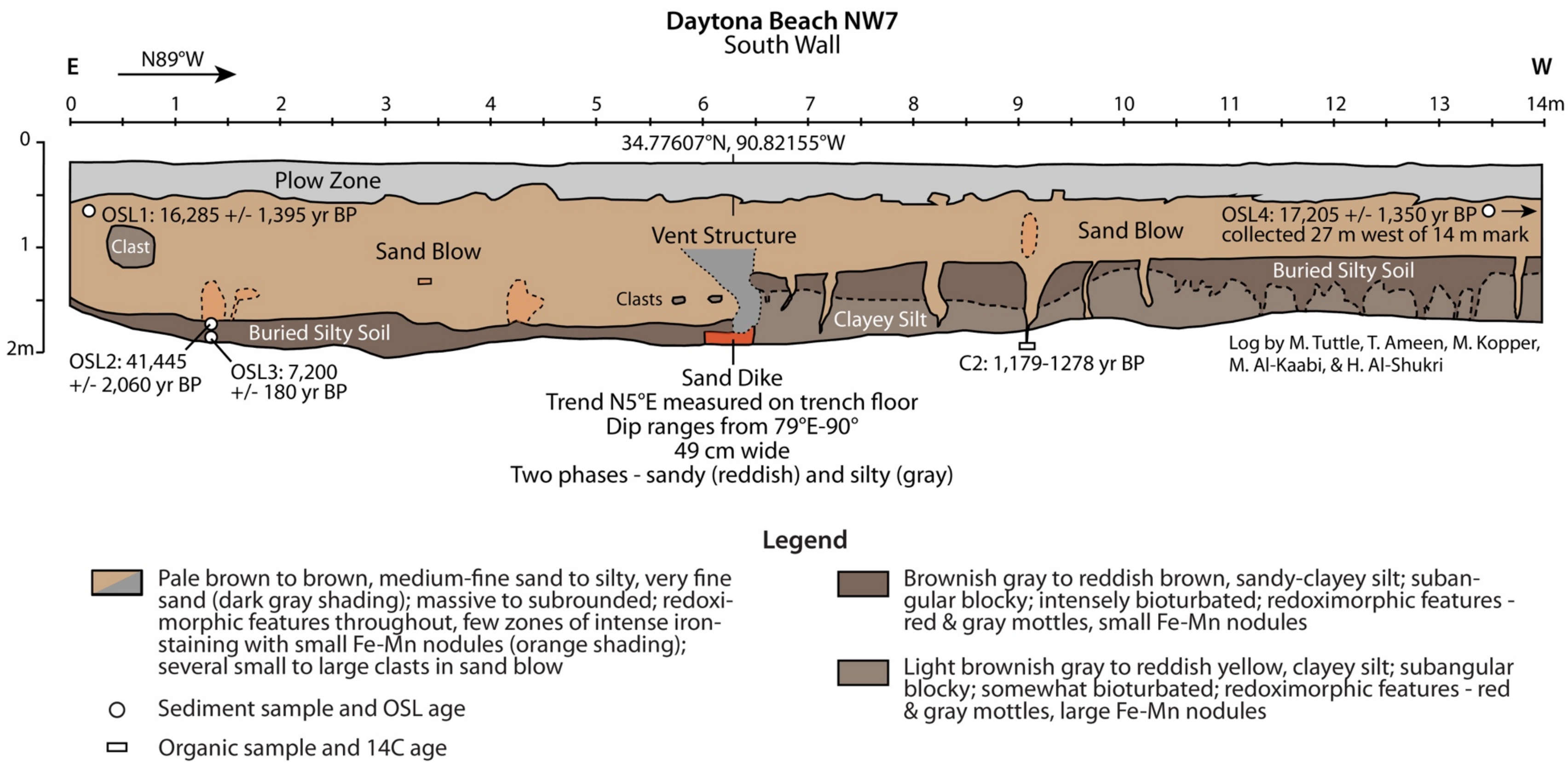

Figure 8. Log of the south wall of the trench excavated in the sand blow at site DBNW7. The trench was excavated close to the transect of GPR profile 156 (see Figures 6 and 7) and shows a cross section of the sand blow, sand dike, buried soils, and the positions of ^{14}C and OSL samples. The sand blow and sand dike were very weathered. C2 collected from a root cast grown through the sand blow and into the buried soils provides a minimum constraining age of about 1179 yr B.P. OSL3 collected 15 cm below the top of the buried soil provides a maximum constraining age of 7,200 ± 180 yr B.P. for the liquefaction features. The age of OSL3 is similar to that of OSL 4 from DBNW5 collected 16 cm below the buried soil. Therefore, it seems likely that the liquefaction features at DBNW7 formed during the same event as the liquefaction features at DBNW5 or about 5.4 ka.

Daytona Beach Northwest 8 Site (DBNW8)

GPS Location of trench: 34.7695°N, 90.8546°W

Observations from GE satellite image and geophysical profiles (Figures 9 and 10):

Width of Sand Blow: 65+ m

Length of Sand Blow: 75 m

Observations from trench (Figure 11):

Thickness of Sand Blow: 1.05 m including plow zone

Width of Sand Dikes: western dike: 54 cm; eastern compound dike: 50 cm and 16 cm

Weathering Characteristics: Sand blow is very weathered with redoximorphic features common and few areas of intense iron staining. Few soil lamellae developed in sand blow

Other Notable Features: Few clasts of clayey silt in and above sand dikes. Flow structure in and above eastern sand dike. Compound sand dike: earlier phase composed of coarse-medium-fine sand; later phase composed of silty, medium-fine sand. The buried soil is displaced downward about 0.3 m on the west side of the eastern dike.

Constraining Ages of Sand Blow from trench (Figure 11; Table 5):

OSL dating of sample OSL5 collected about 8 cm below the top of the buried soil yielded an age of 6,335 ± 150 yr B.P., which represents a maximum constraining age for the sand blow and related sand dikes. There is confidence in the age estimate for OSL5 given its small uncertainty and low overdispersion value of 4 ± 1. Similarly, there is confidence in the age estimate of 14,985 ± 365 yr B.P. for sample OSL6 collected 30 cm below OSL5 from the subsoil.

At nearby site DBNW5, OSL3 (5,110 ± 120 yr B.P.) and OSL 4 (7,475 ± 235 yr B.P) were collected at the top of the buried soil and 16 cm below the sand blow, respectively. At site DBNW8, sample OSL5 was collected 8 cm below the top of the buried soil, or about half the depth between OSL3 and OSL4 at DBNW5. Therefore, it seems likely that the sand blow at DBNW8 formed during the same event or about 5.4 ka.

OSL dating of samples OSL1 and OSL4 collected from the upper part of the sand blow yielded ages of 18,375 ± 495 yr B.P. and 18,605 1,345 yr B.P. and had high dispersion values of 40 ± 8 and 36 ± 6, respectively. Like the samples collected from the upper part of the sand blow at DBNW7, these ages seem much too old and may be due to partial resetting of grain luminescence during rapid deposition of sand vented from below as the result of earthquake-induced liquefaction.

Age Estimate: 5.4 (range 5,327-5,476); based on dating at DBNW8 and nearby DBNW5)

Figure 9. Google Earth satellite image acquired October 2014 of site DBNW8 showing a very large sand blow (light-colored soils), locations of ground-penetrating radar (GPR) profiles 3-9 (yellow lines), and locations of one paleoseismic trench (heavy black line).

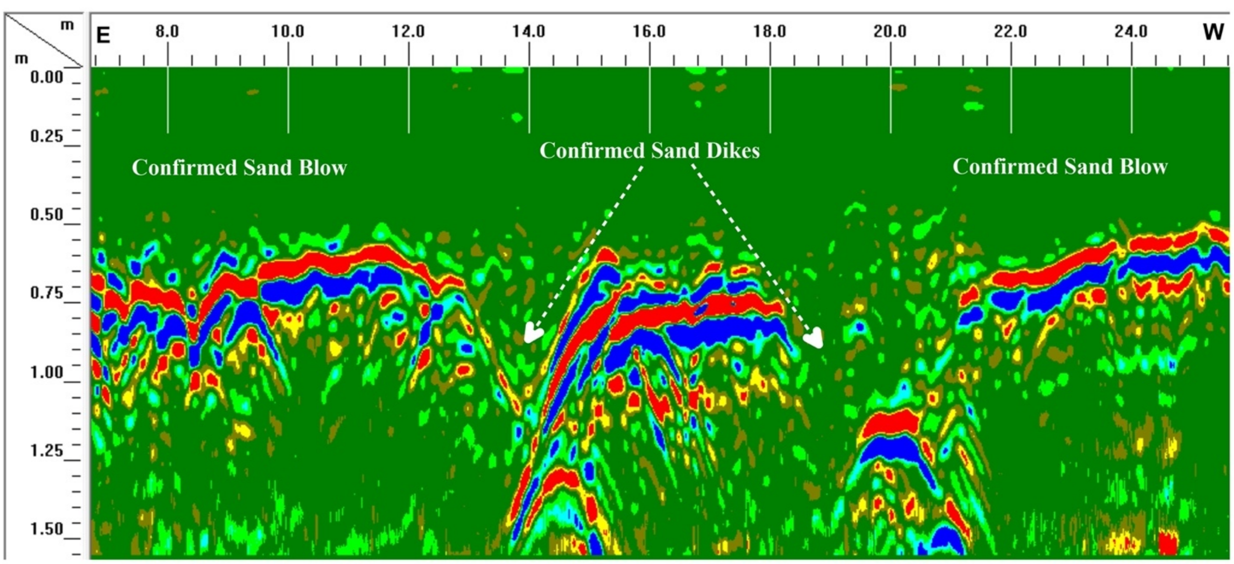

Figure 10. GPR profile 8 shows deformation of a strong reflector (red and blue bands) which represents the contact between the sand blow above and buried silty soil below. A sand blow and two related sand dikes were confirmed in the paleoseismic trench.

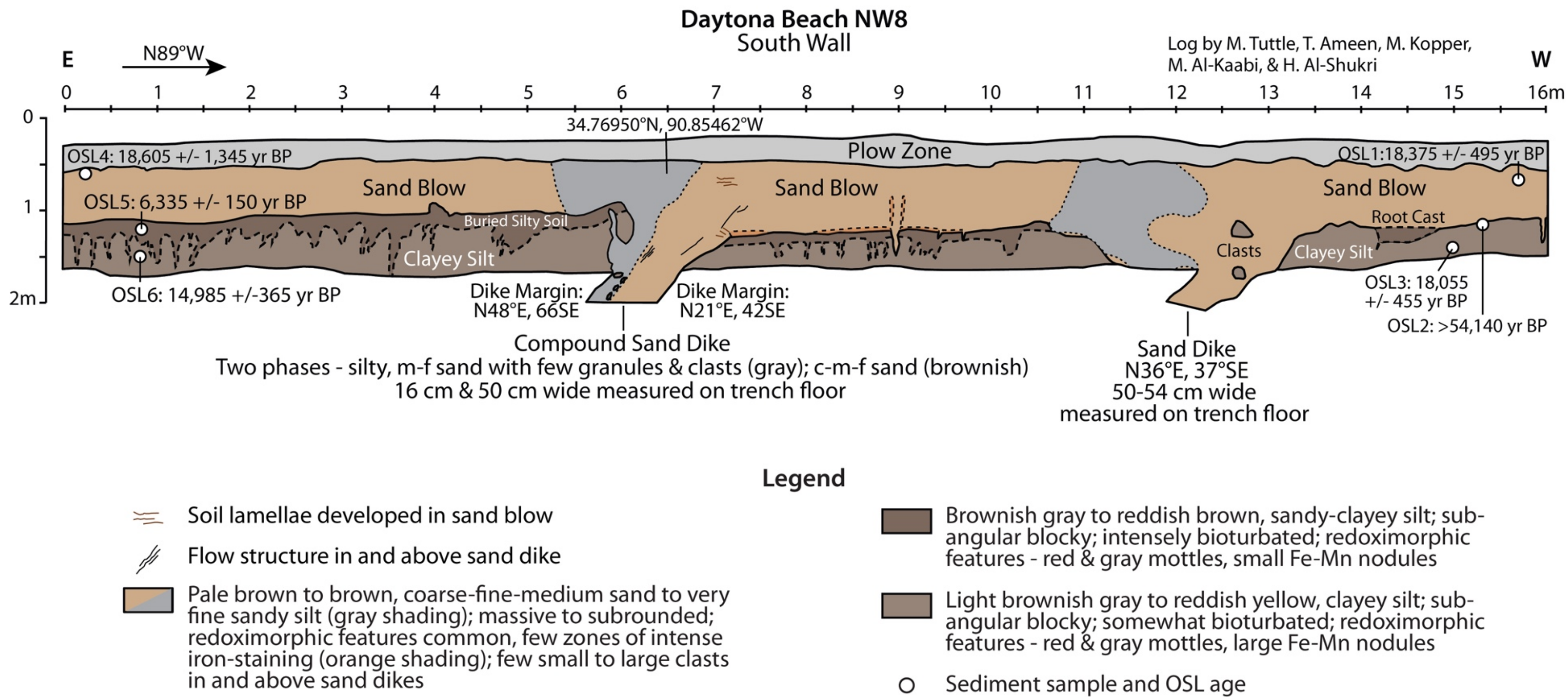

Figure 11. Log of the south wall of the trench excavated in the sand blow at site DBNW8. The trench was excavated close to the transect of GPR profile 8 (see Figures 9 and 10) and shows a cross section of the sand blow, sand dikes, and buried soils, as well as the positions of OSL samples. The sand blow and sand dikes were very weathered. OSL5 collected 8 cm below the top of the buried soil provides a maximum constraining age of 6,485 yr B.P. for the liquefaction features. Given the depth of OSL5 below the top of the buried soil, it seems likely that the liquefaction features at this site formed during the same event as the liquefaction features at nearby site DBNW5 or about 5.4 ka.

Daytona Beach Southeast 2 Site (DBSE2)

GPS Location, Triple Crown trench: 34.7051° N, 90.8011°W

Observations from Google Earth (GE) satellite image and geophysical profiles (Figures 12-14)

Width of Sand Blow: 60 m

Length of Sand Blow: 140 m

Observations from Triple Crown trench (Figures 15 and 16):

Width of Sand Blow: 56+ m

Thickness of Sand Blow: 2.2 m including plow zone

Width of Sand Dikes: 7-130 cm, possibly up to 5+ m

Weathering Characteristics: Weathering, including iron-staining and formation of redoximorphic features and few Fe-Mn nodules, occurs throughout entire thickness of sand blow, but is especially pronounced in the upper 1 m; soil lamellae had formed along margins of dikes; also, fines had accumulated in the lower part of the sand blow above the buried soil and in several of the dikes.

Other Notable Features: A soft-sediment fault occurs adjacent to the western margin of a sand dike and is subparallel to the Daytona Beach lineament. Soil lamellae appear to have been dragged along and offset across the fault (Figure 16). Apparent vertical offset of soil lamellae and mismatch of lamellae thickness across the fault suggest reverse and strike-slip components of displacement.

Constraining Ages (Figure 15; Tables 1 and 2):

^{14}C dating of sample C1 of charred material collected from the top of the soil buried by the large sand blow yielded an age of 9,680-9,910 yr B.P. This represents a close maximum constraining age for the sand blow, indicating that it formed about 9.8 ka. OSL dating of sample OSL1 collected from the buried soil near sample C1 and within 5 cm of the base of the sand blow yielded an age of 11,940 ± 1,000. The age for sample OSL1 is consistent with the younger age for C1 collected higher in the buried soil.

Age Estimate: 9.8 ka (range 9,680-9,910 yr B.P.)

Reference: Al-Shukri, H., Mahdi, H., Al-Qadhi, O., and Tuttle, M.P., 2009, Spatial and temporal characteristics of paleoseismic features in the southern terminus of the New Madrid seismic zone in eastern Arkansas, Final Technical Report, Prepared for U.S. Geological Survey award 1434-07HQGR0069, 24 p.

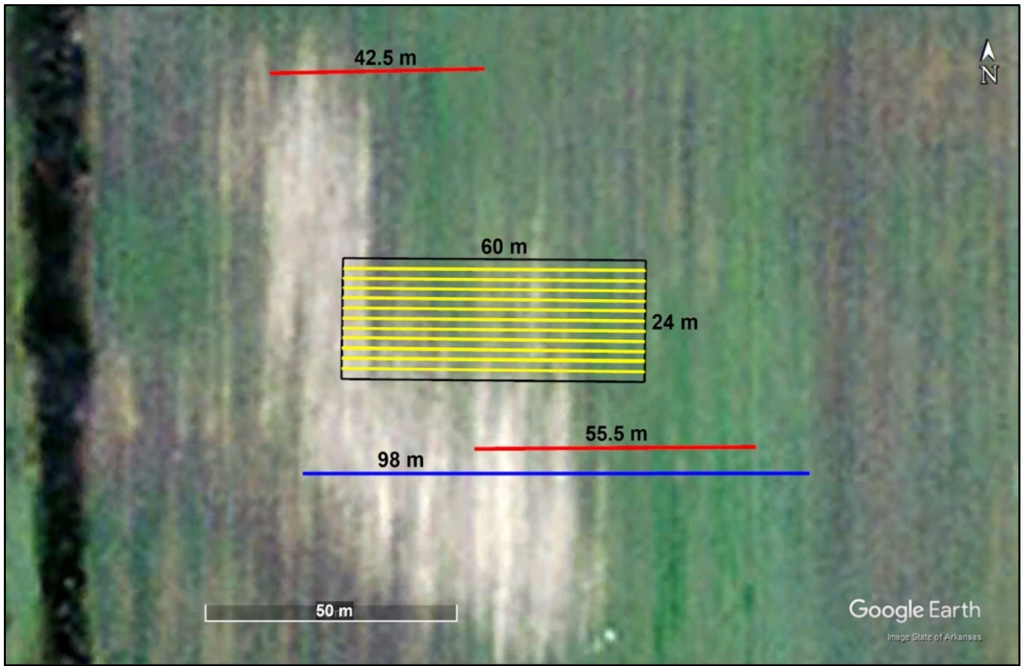

Figure 12. GE satellite image acquired January 2006, showing light-colored sand blow at DBSE2 site, locations of ground-penetrating radar (GPR) profiles (yellow lines within black rectangular area), resistivity profile (blue line), and paleoseismic trenches (red lines).

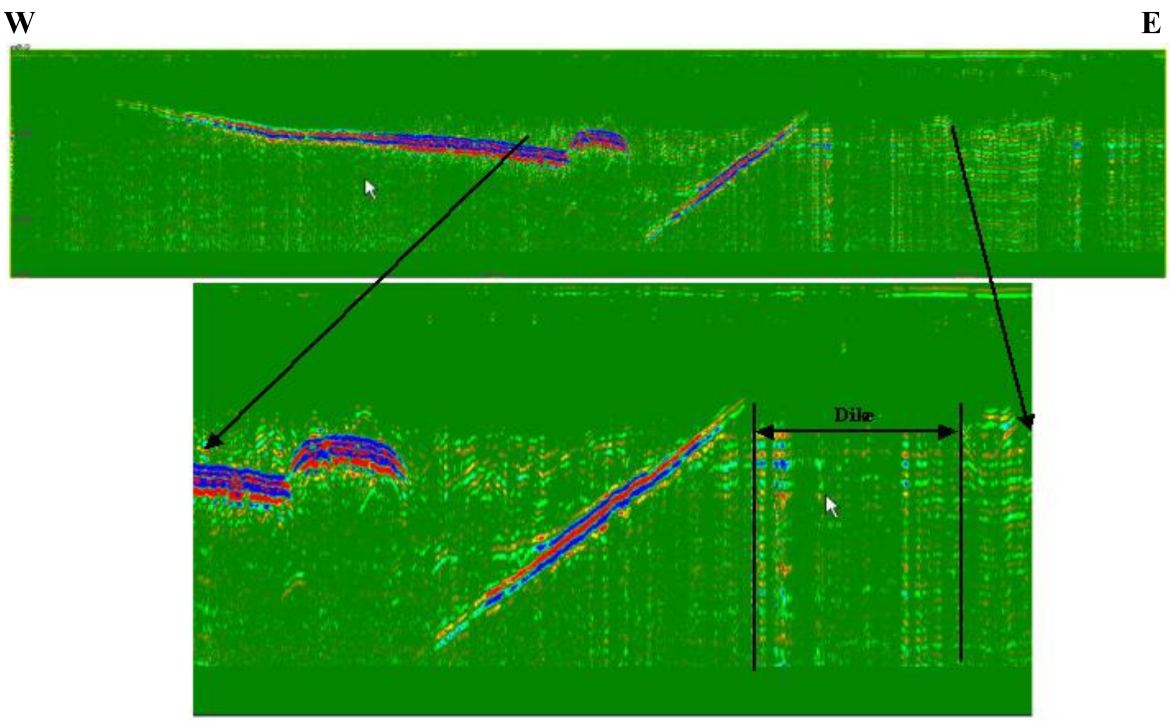

Figure 13. GPR profiles showing subsurface anomalies related to sand blows. (Upper) The red and blue color bands represent the contact between sand blow above and buried soil below. The paleo ground surface suffered significant deformation, including subsidence and tilting of large blocks. (Lower) Blowup of central portion of the profile, as indicated by black arrows. Sand dikes formed between the deformed blocks of soil.

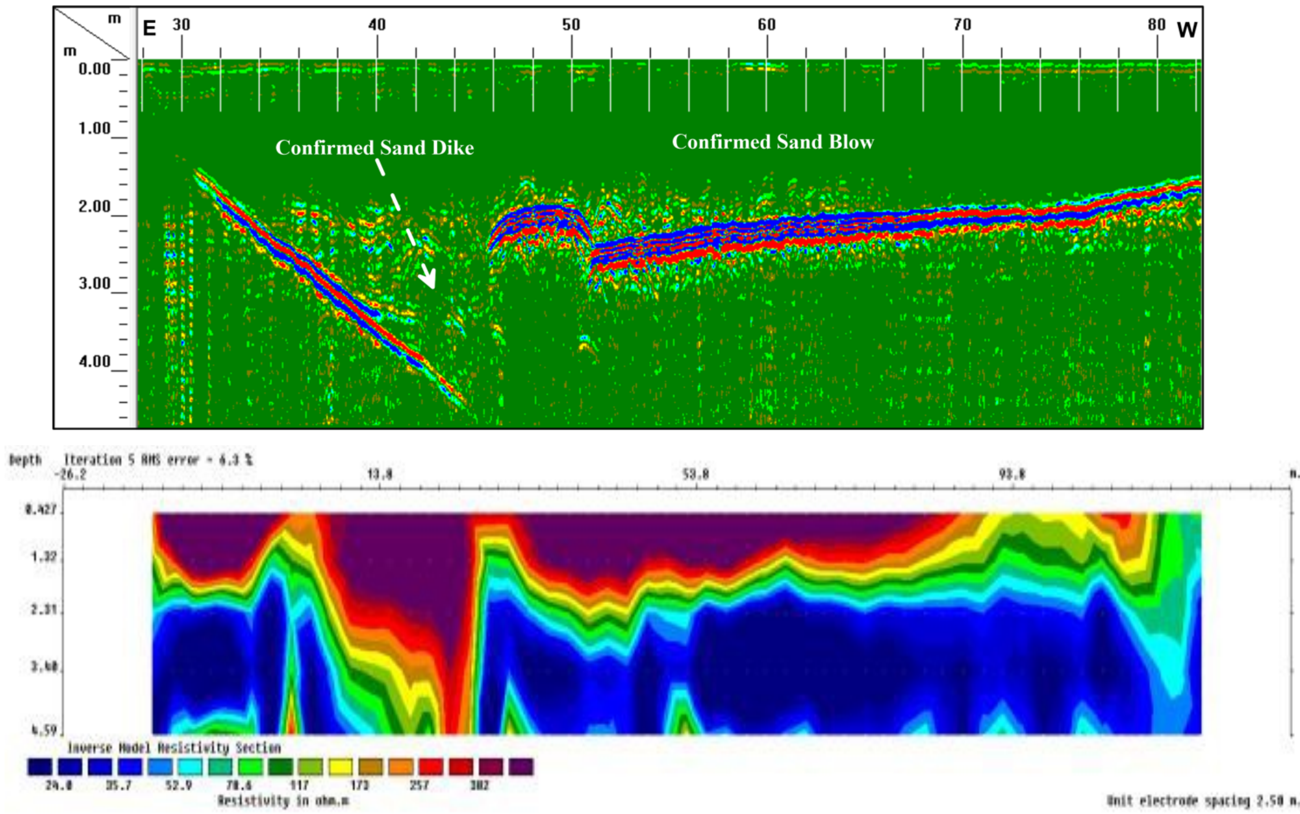

Figure 14. (Upper) Same GPR profile as shown in Figure 13 but reversed. (Lower) resistivity profile at the same site. The high resistivity values correspond with the sand blow and sand dikes. The strongest subvertical anomaly corresponds with the large sand dike indicated on the GPR profile.

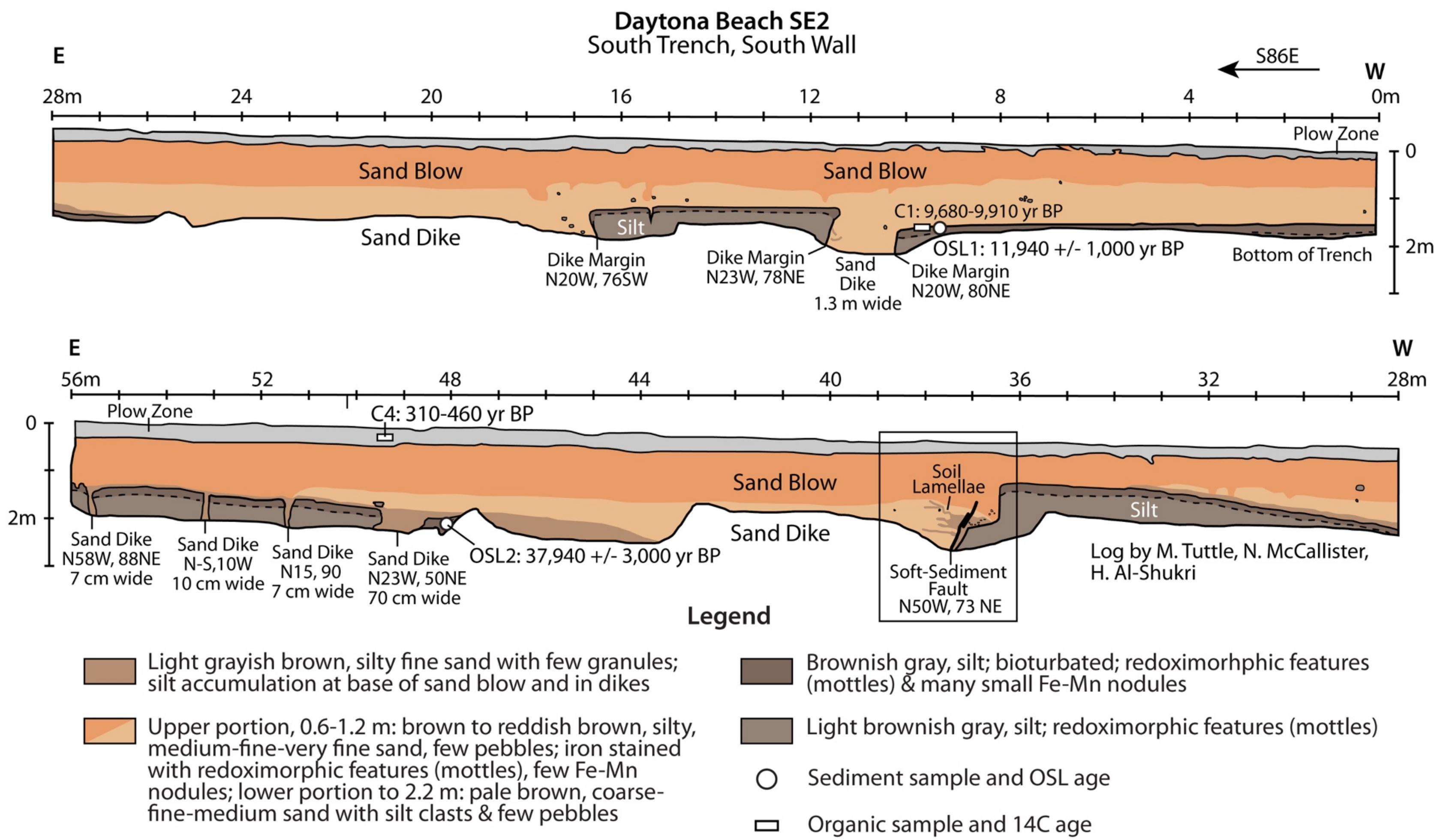

Figure 15. Log of the south wall of the Triple Crown trench excavated at site DBSE2 showing a cross-section of the sand blow, sand dikes, and buried soils, as well as the positions of samples collected for ^{14}C and OSL dating. Dating of the buried soil provides close maximum constraining ages for the sand blow and related dikes, indicating that they formed about 9.8 ka. Note that the upper 0.6-1.2 m of the sand blow is very weathered (indicated by reddish brown shading), that silt has accumulated along the bottom of the sand blow, and that soil lamellae have formed in the sand dikes. Location of the trench is shown on Figure 12.

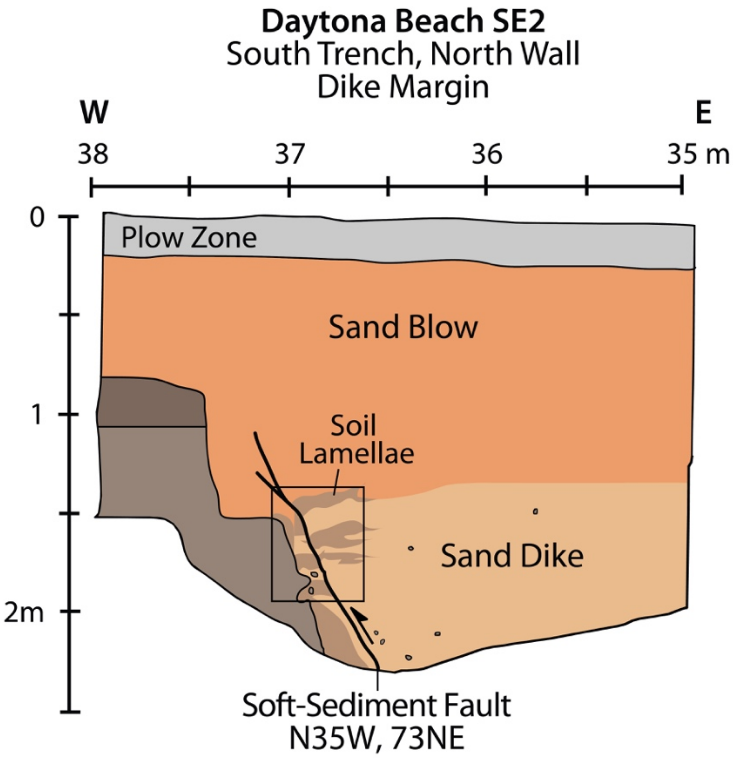

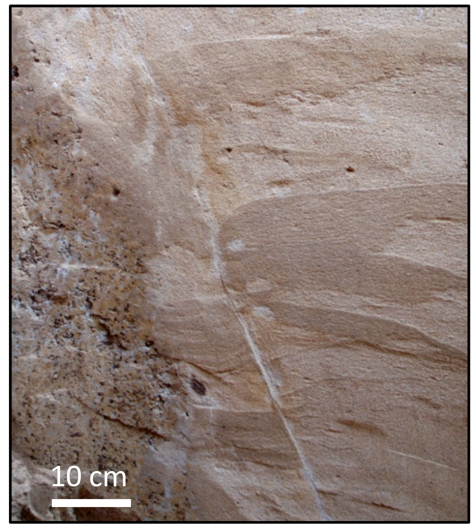

Figure 16. (Left) Portion of log of the north wall of Triple Crown trench at site DBNW2 showing the western margin of a sand dike along which soil lamellae appear to have been dragged along and offset by a soft-sediment fault with a strike and dip of N35°W, 73°NE. The dike margin and fault were traced across the trench floor to the south wall of the trench and are outlined on Figure 15 with a rectangle (also see Figure 15 for unit descriptions). The fault parallels the Dayton Beach lineament. (Right) Photograph of soft-sediment fault along which soil lamellae are dragged and offset. Vertical offset of soil lamellae and mismatch of lamellae thickness across the fault suggest reverse and strike-slip components of displacement. Area of the photograph is outlined on the adjacent log with a rectangle.

Daytona Beach Northwest 2 Site (DBNW2)

GPS Locations:

South trench: 34.7271° N, 90.8176°W

North trench: 34.7274° N, 90.8181°W

Observations from GE satellite image and geophysical profiles (Figures 17 and 18):

Width of Sand Blow: 100+ m

Length of Sand Blow: 300+ m

Observations from South trench (Figure 19):

Width of Sand Blow: 13+ m; sand blow extends >7 m west of dike

Thickness of Sand Blow: 1.6 m including plow zone

Width of Sand Dike: 6.4 m

Weathering Characteristics: The upper 0.5 m of the sand blow is very weathered, including redoximorphic features (mottles) and manganese staining. Silt has accumulated and a few soil lamellae formed along the eastern margin of the dike.

Other Notable Features: The soil below the large sand blow, which represents the event horizon, is displaced downward about 1.5 m on the west side of the dike.

Constraining Ages of Sand Blow from South trench (Figure 19 and Table 3):

OSL dating of samples OSL1 and OSL2 collected from the buried soil below the sand blow yielded ages of 15,040 ± 4,540 yr B.P. and 19,540 ± 1,010 yr B.P., respectively. Although the samples were collected from the same context, their ages are quite different from one another and both have large uncertainties. Also, overdispersion values are high suggesting that the samples were of mixed sediment or poorly bleached. Therefore, these ages reflect maximum ages, but not close maximum ages. Based on the younger of the two results, the sand blow may have formed less than 15 ka.

Observations from North trench (Figure 20):

Width of Sand Blow: 14+ m as observed in trench; sand blow extends >7 m west of dike

Thickness of Sand Blow: 2.4 m including plow zone

Width of Sand Dike: 4.5 m

Weathering Characteristics: The entire sand blow is extremely weathered, including iron-staining and formation of redoximorphic features, but especially the upper 1 m of the sand blow. Silt accumulated along the base of the sand blow above the buried soil and a 1.5 m thick sequence of soil lamellae formed along the eastern margin of the large dike.

Other Notable Features: Flow structure in the sand blow above the dike. The soil below the large sand blow is displaced downward about 1.2 m on the west side of the dike. Two soft-sediment faults, adjacent to the eastern margin of a sand dike, appear to offset the sequence of soil lamellae. In addition, several domains of relatively unweathered, loose sand appear to have been injected along the faults. These observations suggest that a second event, including faulting and earthquake-induced liquefaction, occurred thousands of years after the first event responsible for the formation of the large sand blow and dike. The second event may be the same event responsible for the large sand blow in the South trench.

Constraining Ages of Sand Blow from North trench (Figure 20 and Table 3):

OSL dating of samples OSL2 and OSL1 collected from the buried soil below the sand blow yielded ages of 24,340 ± 1,790 yr B.P. and 32,440 ± 1,880 yr B.P., respectively. Although the samples were collected from the same context, their ages are quite different from one another and both have large uncertainties. Again, overdispersion values are high suggesting that the samples were of mixed sediment or poorly bleached. Therefore, these ages reflect maximum ages, but not close maximum ages. Based on the younger of the two results, the sand blow may have formed less than 24.3 ka.

Age Estimates: 15 ka (range 10,500-19,580 yr B.P.) sand blow in south trench; 24.3 ka (range 22,550-26,130 yr B.P.) sand blow in north trench. The two trenches are about 50 m apart and both cross the northwest trend of the large sand dikes. The sand blows documented in the two trenches appear to have formed along the same structure but during two different events separated by thousands of years. The site was revisited to collect additional samples to better constrain the age of the sand blow(s). Unfortunately, the site had been excavated and the sand blow(s) removed for building materials.

Reference: Al-Shukri, H., Mahdi, H., Tuttle, M. P., Dyer-Williams, K., 2015, Geophysical and paleoseismic investigations of large sand blows along a northwest-oriented lineament near Marianna, Arkansas, Final Technical Report, Prepared for U.S. Geological Survey award G12AP20093, 31 p.

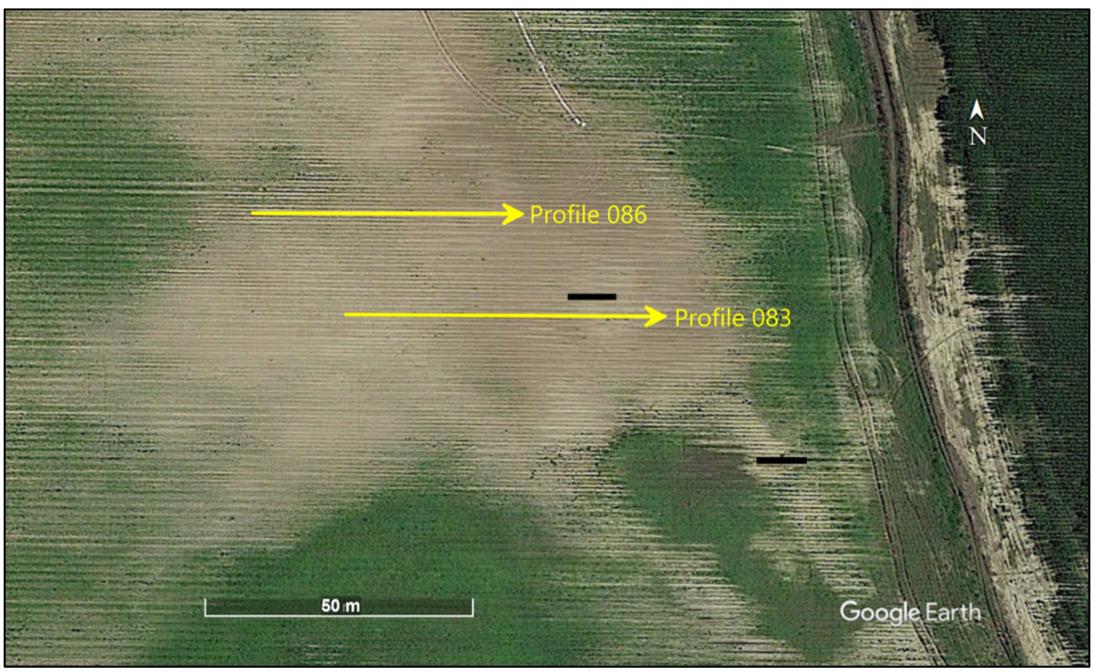

Figure 17. Google Earth satellite image acquired June 2016 showing the very large sand blow (light-colored soils) at site DBNW2, locations of two of the GPR profiles (yellow lines), and locations of the southern and northern paleoseismic trenches (heavy black lines).

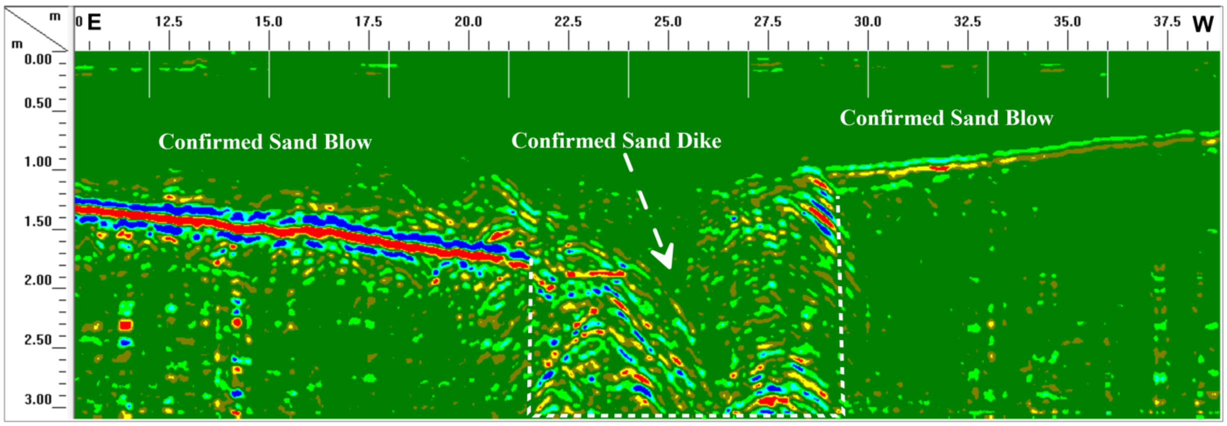

Figure 18. GPR profile 086 shows deformation of a strong reflector (red and blue bands) which represents the contact between the sand blow above and buried silty soil below. A 6.4 m-wide discontinuity in the contact is due to a large dike that crosscuts the soil.

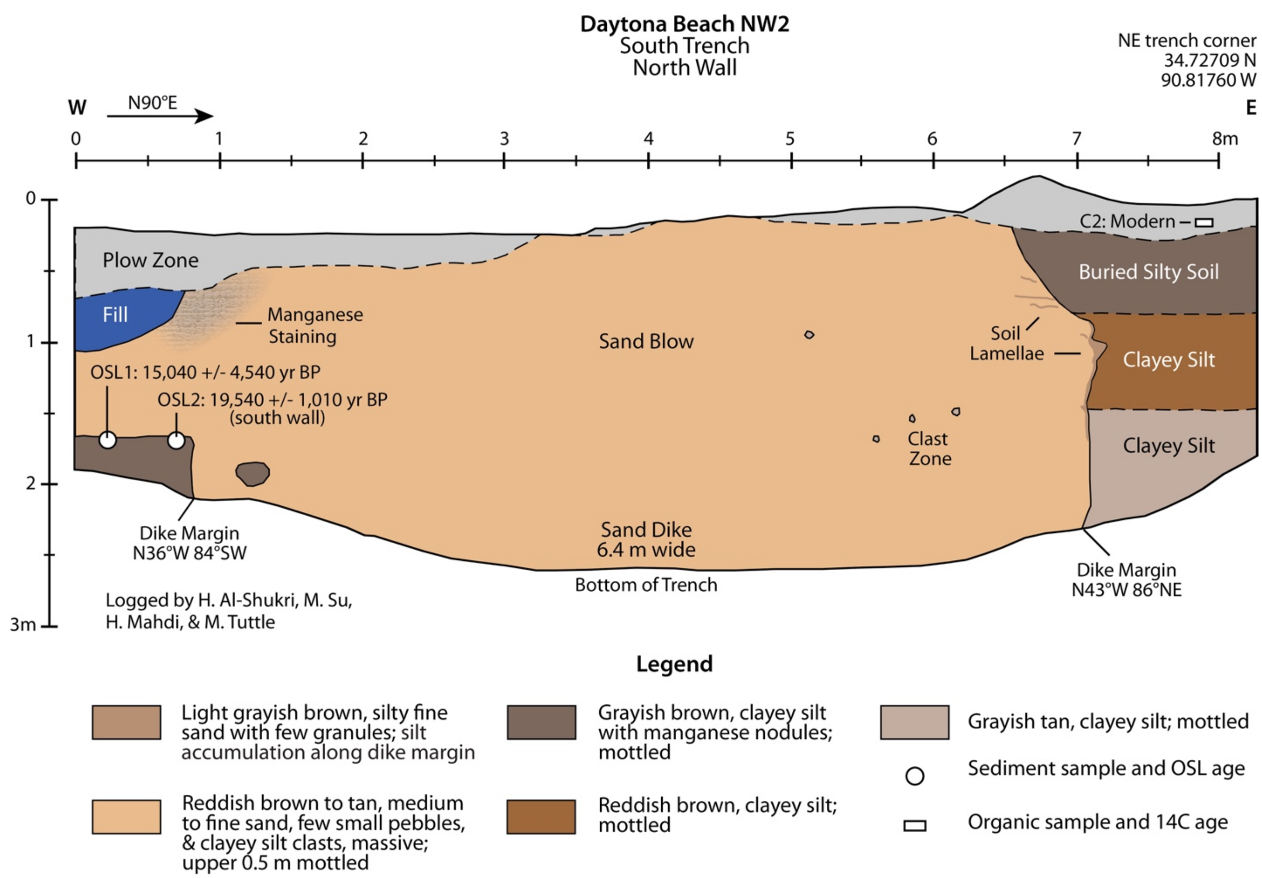

Figure 19. Log of the north wall of the southern trench at site DBNW2. This sand blow and dike exhibit iron staining, silt accumulation, and formation of soil lamellae. However, they are less weathered than the sand blow and dike in the northern trench, suggesting that they may be younger in age. OSL1, collected slightly higher in the buried soil than OSL2, gave a younger age of 15,040 ± 4,540 yr B.P. However, the ages of both samples are very different from one another and had large error ranges leading to lack of confidence in the results.

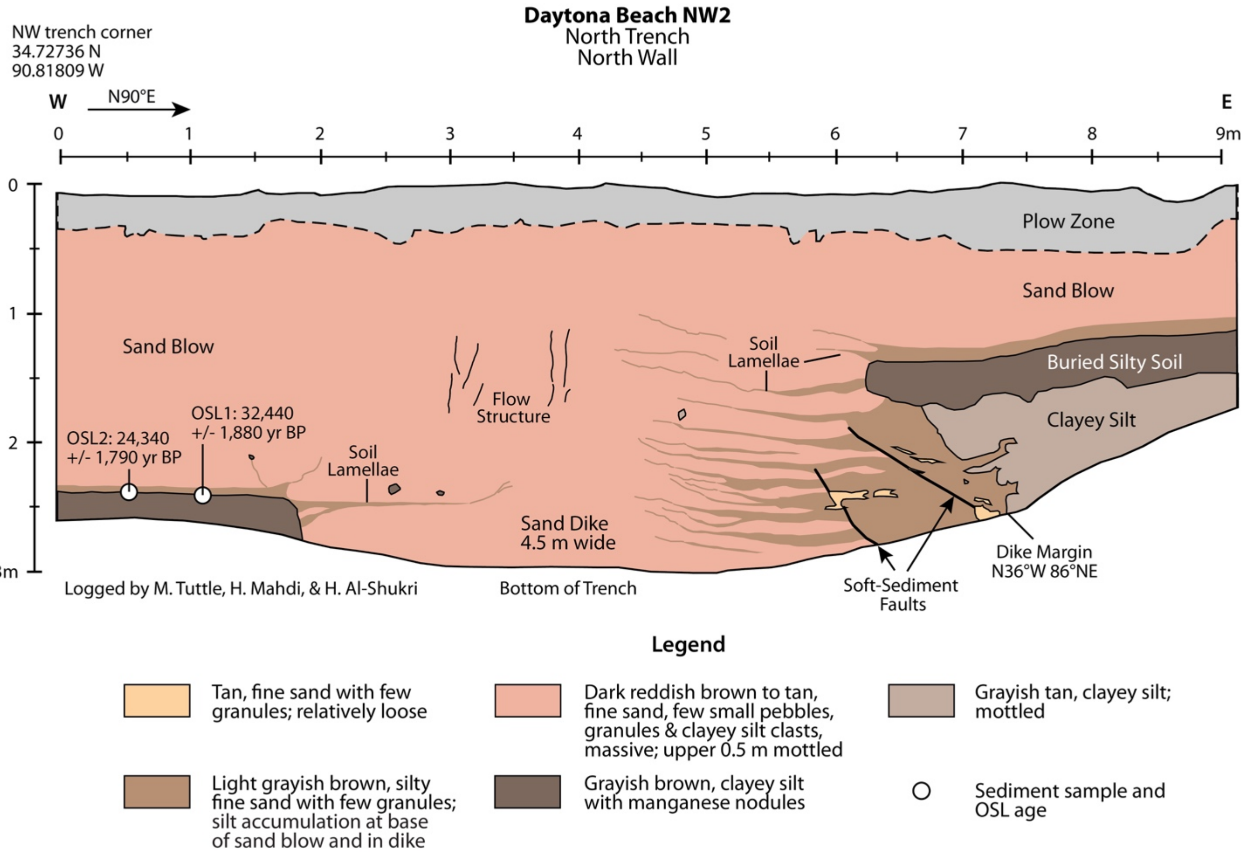

Figure 20. Log of the north wall of the north trench at site DBNW2. This sand blow and dike are extremely weathered with silt accumulation above the buried soil and formation of soil lamellae within the dike. The lamellae appear to be offset by soft-sediment faults along which dikes of loose fine sand may have been injected, suggesting a subsequent event. OSL2, collected slightly higher in the buried soil than OSL1, gave a younger age of 24,340 ± 1,790 yr B.P. Again, the ages of both samples are very different from one another and had large error ranges leading to lack of confidence in the results.

Daytona Beach Northwest 3 Site (DBNW3)

GPS Locations:

North trench: 34.7312° N, 90.8206°W
South trench: 34.7311° N, 90.8205°W

Observations from GE satellite image and geophysical profiles (Figures 21 and 22):

Width of Sand Blow: 52 m from GPR survey
Length of Sand Blow: 85 m from GPR survey

Observations from North trench (Figure 23):

Thickness of Sand Blow: 75 cm including plow zone

Width of Sand Dikes: 17 cm and 4 cm

Weathering Characteristics: Iron staining in upper 55-65 cm of sand blow and upper 15-25 cm of sand dike; also, several Fe-Mn nodules and soil lamellae had formed in upper 50 cm of sand blow.

Other Notable Features: The buried soil below the large sand blow is tilted such that it is 40 cm lower at the east end of the trench than at the west of the trench. The buried soil may be displaced downward about 10 cm on the east side of the dike.

Constraining Ages of Sand Blow from North trench (Figure 23 and Table 1 and 4):

^{14}C dating of sample C1 of charred material from the buried soil about 13 cm below the sand blow yielded an age of 4,573-4,805 yr B.P. This represents a fairly close maximum constraining age of 4.7 ka for the sand blow. OSL dating of sample OSL1 collected from the buried soil 3-5 cm below the sand blow yielded an age of 4,710 ± 215 yr B.P. This age is consistent with the ^{14}C age of C1 and supports the age estimate of 4.7 ka for the sand blow. Sample OSL3 collected from the subsoil 33-38 cm below the sand blow yielded an age of 13,310 ± 540 yr B.P. Again, the OSL age had fairly low dispersion value lending confidence in the age.

Observations from South trench (Figure 24):

Thickness of Sand Blow: 100 cm including plow zone

Width of Sand Dike: 72 cm in north wall; 100 cm in south trench

Weathering Characteristics: Iron staining in upper 70-90 cm of sand blow and upper 15 cm of sand dike; also, several Fe-Mn nodules and soil lamellae had formed in upper 50 cm of sand blow.

Other Notable Feature: The soil below the large sand blow is displaced downward about 40 cm on the east side of the dike.

Constraining Ages of Sand Blow from South trench (Figure 24 and Table 4):

Sample OSL1 collected from the subsoil 32-37 cm below the sand blow yielded an age of 12,500 ± 405 yr B.P., very similar to the age of OSL3 collected from a similar context in the northern trench. The OSL age had fairly low dispersion value suggesting that the sediment was not mixed, lending confidence in the age estimate of the soil.

Age Estimate: 4.7 ka; (range 4,573-4,805 yr B.P.). The two trenches are about 10 m apart and both cross the northwest trend of a through-going sand dike. The sand blow documented in the two trenches is one and the same and formed during one event about 4.7 ka.

Reference: Tuttle M. P., Al-Shukri, H, and Mahdi, H., 2020, Geophysical and paleoseismic investigations of large sand blows along a northwest-oriented lineament near Marianna, Arkansas, Final Technical Report, U.S. Geological Survey award G18AP00083, 31 p.

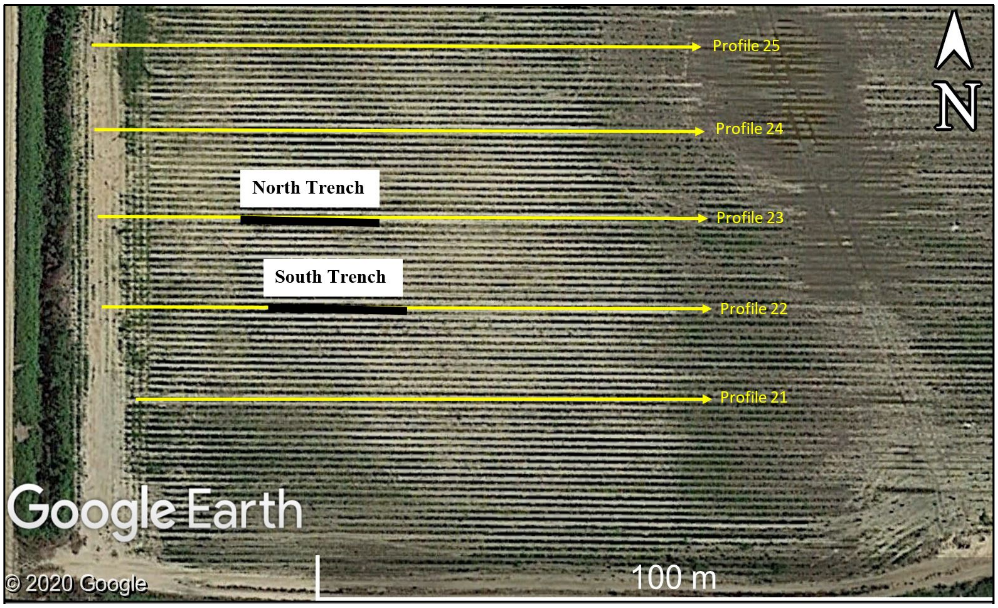

Figure 21. Google Earth satellite image acquired June 2016 showing the northwest-southeast elongated sand blow (light-colored soils) at site DBNW3, locations of GPR profiles 21, 22, 23, 24, and 25 (yellow lines), and locations of two paleoseismic trenches (heavy black lines).

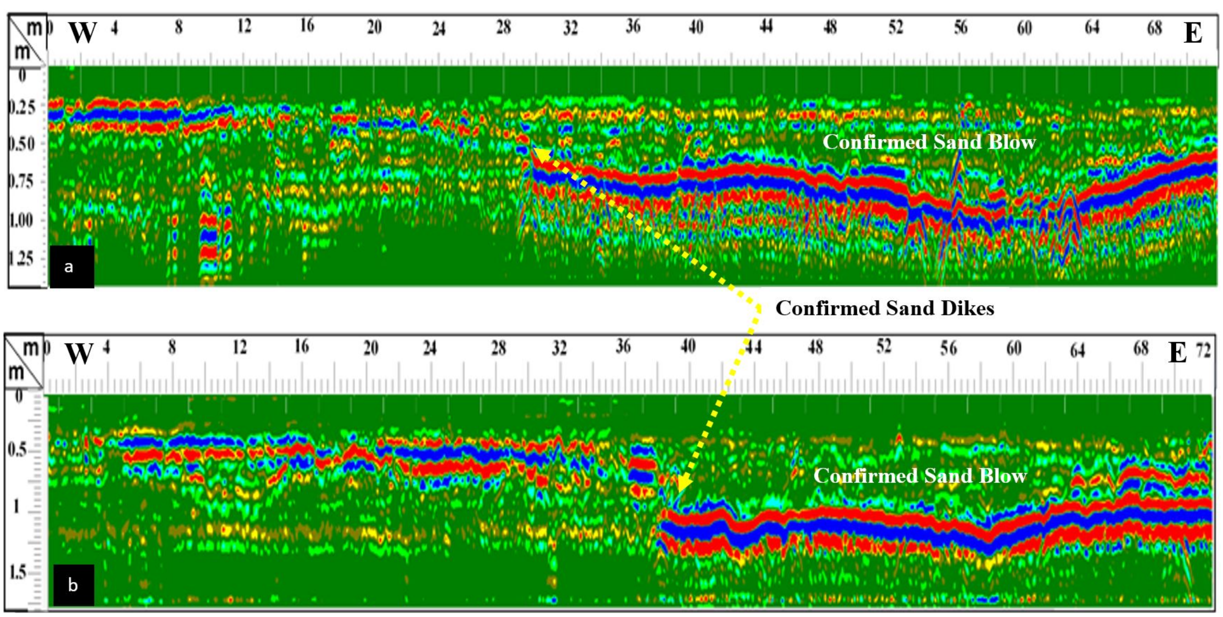

Figure 22. GPR profiles 23 (upper) and 22 (lower) show deformation of a strong reflector (red and blue bands) which represents the contact between the sand blow above and buried silty soil below. Discontinuities in the contact are related to ground failure and dike emplacement.

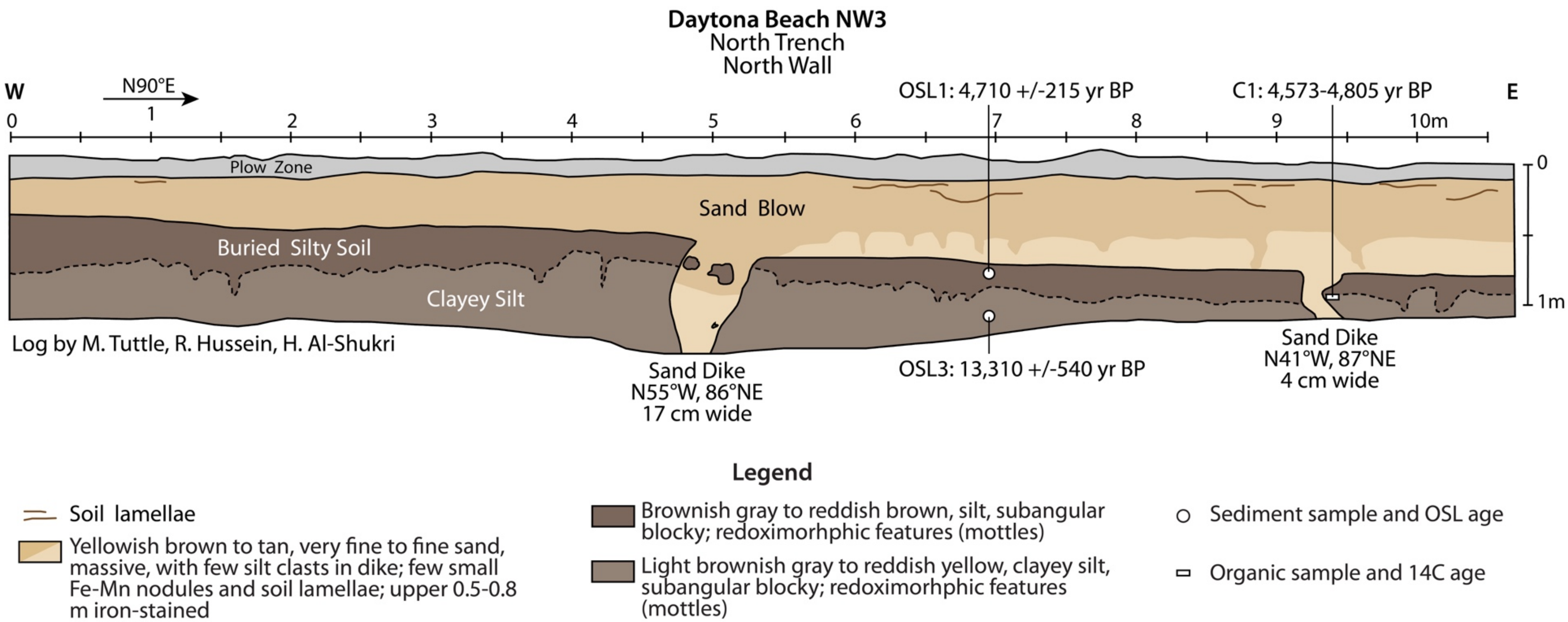

Figure 23. Log of the north wall of the northern trench excavated in the sand blow at site DBNW3. The trench was excavated along the transect of GPR profile 23 (see Figures 21 and 22) and shows a cross-section of the sand blow, sand dikes, and buried soils, as well as the positions of OSL and ^{14}C samples. ^{14}C and OSL dating of the buried soils provides close maximum constraining ages for the sand blow and related sand dikes and indicate that they formed about 4.7 ka. Note that the upper 0.5-0.8 m of the sand blow is weathered (indicated by light brown shading) and includes small Fe-Mn nodules and soil lamellae.

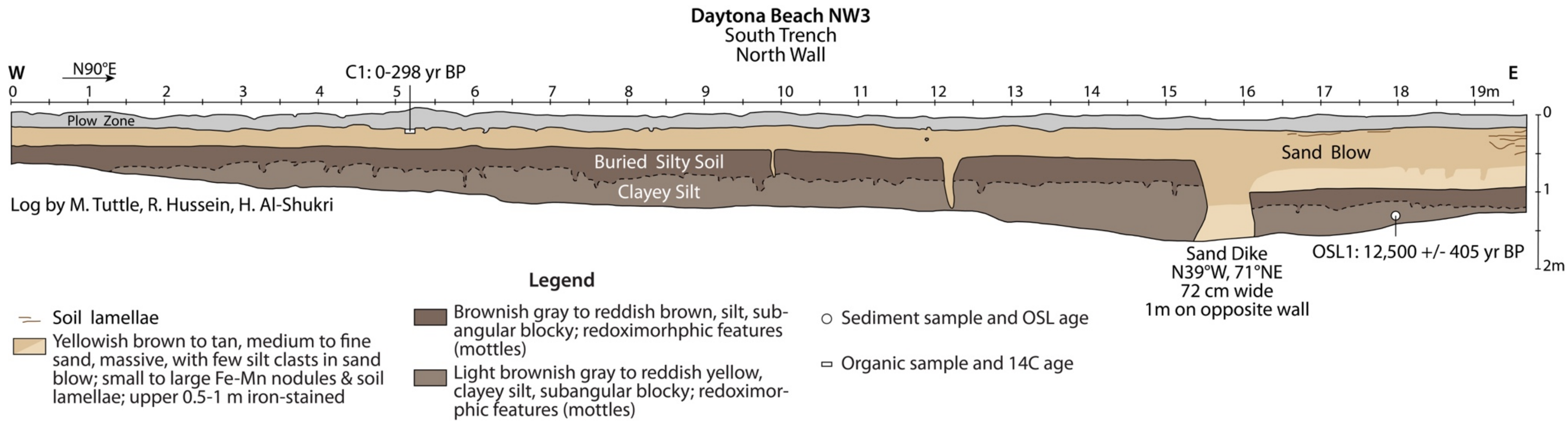

Figure 24. Log of the north wall of the southern trench excavated in the sand blow at site DBNW3. The trench was excavated along the transect of GPR profile 22 (see Figures 21 and 22) and shows a cross-section of the sand blow, sand dike, and buried soils, as well as the position of OSL and ^{14}C samples. OSL date of the buried subsoil (OSL1) agrees with the date of the buried subsoil (OSL3) in the northern trench. The organic sample (C1) collected immediately below the plow zone from the upper part of the sand blow is very young and probably was from a root recently grown into the sand blow from above. As in the northern trench, the upper 0.5-0.8 m of the sand blow is weathered (indicated by light brown shading) and includes small Fe-Mn nodules and soil lamellae.

Table 1. Results of radiocarbon dating of charred material and organic sediment associated with sand blows (2010-2023).

Trench Sample # Beta #	$^{13}C/^{12}C$ Ratio[a]	Conventional ^{14}C Age Yr B.P.[b]	Calibrated Age Yr B.P.[c] 1-sigma	Calibrated Calendar Date[c] 1-sigma	Prob. %	Calibrated Age Yr B.P.[c] 2-sigma	Calibrated Calendar Date[c] 2-sigma	Prob. %	Sample Description[d]
SITE DBSE2									
Triple Cr. C1 252610	NA	8780 ± 60	9680-9910	7730-7960 BC	68	9560-9960 9990-10150	7610-8010 BC 8040-8200 BC	95	Charred material, buried soil below sand blow
Triple Cr. C4 276429	NA	320 ± 40	310-460	AD 1640-1490	68	290-490	AD 1660-1460	95	Charred material, base of plow zone above sand blow
SITE DBNW3									
North C1 546853	-24.1	4120 ± 30	4573-4647 4760-4805 4674-4696	2624-2698 BC 2811-2856 BC 2725-2747 BC	36.7 21.3 10.2	4528-4726 4753-4815	2579-2777 BC 2804-2866 BC	70.3 25.1	Charred material, buried soil, collected ~13 cm below sand blow
South C1 546854	-23.8	210 ± 30	150-185 272-298 Post BP 0-10	AD 1800-1765 AD 1678-1652 Post AD 1950-1940	33 25 10.2	144-216 266-304 Post BP 0-21	AD 1806-1734 AD 1684-1646 Post AD 1950-1929	50.5 30.8 14.1	Charred material, near the contact of the plow zone and sand blow
SITE DBNW5									
South C1 546855	-24.3	710 ± 30	656-683	AD 1294-1267	68.2	644-694 565-588	AD 1306-1256 AD 1385-1362	84.8 10.6	Charred material, tree root cast in upper part of sand blow
South SL1 681253	-18.0	4760 ± 30	5507-5577 5474-5485	3558-3628 BC 3525-3536 BC	59.7 8.5	5460-5585 5355-5377 5331-5348	3511-3636 BC 3406-3428 BC 3382-3399 BC	87.8 4.2 3.4	Organic sediment, upper 0.5 cm of buried sand blow; near OSL3
South SL2 681254	-17.8	4710 ± 30	5327-5388 5445-5476 5395-5400	3378-3439 BC 3496-3527 BC 3446-3451 BC	44.9 21.1 2.2	5322-5417 5438-5438 5525-5575 5510-5520	3373-3468 BC 3489-3534 BC 3576-3626 BC 3561-3571 BC	54.8 24.1 14.9 1.6	Organic sediment, upper 0.5 cm of buried sand blow; near OSL1
SITE DBNW7									
Tr C2 681255	-25.1	1290 ± 30	1179-1214 1244-1278	AD 771-736 AD 706-672	35.2 33.0	1176-1291	AD 774-659	95.4	Charred material, 175 cm BS near tip of root cast that extends thru sand blow into buried soil

[a] NA – not applicable.

[b] Conventional radiocarbon ages in years B.P. or before present (1950) determined by Beta Analytic, Inc. Errors represent 1 standard deviation statistics or 68% probability.

[c] Calibrated age ranges and calendar dates as determined by Beta Analytic, Inc., using the high probability density range method (Bronk Ramsey, 2009) and INTCAL20 (Reimer et al., 2020). 1-sigma error ranges represent 68.2% probability and 2-sigma ranges represent 95.4% probability.

[d] Abbreviations: OSL – optically stimulated luminescence sample; BS – below surface.

Table 2. Results of optically-stimulated luminescence dating of soils buried by sand blows (2010).

Trench Sample #	H20 (%)[a]	K (%)[b]	U (ppm)[b]	Th (ppm)[b]	Cosmic Dose Additions (Gy/ka)[c]	Total Dose (Gy/ka)	Equivalent Dose (Gy)	n[d]	OSL Age (Yr)[e]	OSL Age Yr. B.P. (AD 1950)	Sample Description
SITE DBSE2											
Triple Cr. OSL1	15 (45)	1.70 ± 0.07	2.25 ± 0.10	7.26 ± 0.2	0.17 ± 0.02	2.56 ± 0.06	30.6 ± 1.83	19 (20)	12,000 ± 1,000	11,940 ± 1,000	Buried soil at contact with sand blow above
Triple Cr. OSL2	12 (35)	1.73 ± 0.08	2.27 ± 0.13	7.26 ± 0.2	0.16 ± 0.01	2.65 ± 0.08	103 ± 3.61	19 (20)	38,000 ± 3,000	37,940 ± 3,000	Buried soil 20 cm below contact with sand blow above
Double Cr. OSL3	16 (30)	1.73 ± 0.07	2.17 ± 0.17	7.26 ± 0.2	0.16 ± 0.01	2.52 ± 0.07	103 ± 3.61	19 (20)	52,000 ± 3,000	51,940 ± 3,000	Buried soil at contact with sand blow above

[a] Field moisture, with figure in parentheses indicating the complete sample saturation %. Ages calculated using approximately 30% of saturation values.

[b] Analyses obtained using low-resolution gamma spectrometry (NaI detector).

[c] Cosmic doses and attenuation with depth were calculated using the methods of Prescott and Hutton (1994).

[d] Number of replicated equivalent dose (De) estimates used to calculate the mean. Figures in parentheses indicate total number of measurements made including failed runs with unusable data.

[e] Dose rate and age for fine-grained 125-90 um quartz sand. Linear + exponential fit used on age, errors to one sigma, weighted mean used. Datum year assumed to be AD 2010. OSL ages determined by U.S. Geological Survey, Denver, CO.

Table 3. Results of optically-stimulated luminescence dating of soils buried by sand blows (8/31/2015).

Trench Sample #	H20 (%)[a]	K (%)[b]	U (ppm)[b]	Th (ppm)[b]	Total Dose (Gy/ka)[d]	Equivalent Dose (Gy)	n[e]	Scatter (%)[f]	OSL Age (Yr)[g]	OSL Age Yr. B.P. (AD 1950)	Sample Description
SITE DBNW2											
North OSL1	12 (26)	1.34 ± 0.03	1.30 ± 0.04	4.50 ± 0.14	2.03 ± 0.06	65.9 ± 3.34	3 (15)	29	32,500 ± 1,880	32,440 ± 1,880	Buried soil at contact with sand blow above
North OSL2	12 (21)	1.01 ± 0.04	0.91 ± 0.11	2.94 ± 0.26	1.54 ± 0.08	37.5 ± 1.97	2 (15)	41	24,400 ± 1,790	24,340 ± 1,790	Buried soil at contact with sand blow above
South OSL1	12 (33)	1.30 ± 0.03[c]	0.90 ± 0.03[c]	3.56 ± 0.18[c]	1.82 ± 0.05	27.5 ± 0.42	2 (14)	42	15,100 ± 4,540	15,040 ± 4,540	Buried soil at contact with sand blow above
South OSL2	13 (21)	1.25 ± 0.03[c]	0.60 ± 0.02[c]	2.80 ± 0.14[c]	1.70 ± 0.04	33.3 ± 1.51	2 (7)	33	19,600 ± 1,010	19,540 ± 1,010	Buried soil at contact with sand blow above

[a] Field moisture, with figure in parentheses indicating the complete sample saturation %. Ages calculated using 25% of the saturated moisture (i.e., 12 (26): 26 * 0.25 = 6).

[b] Analyses obtained using high-resolution gamma spectrometry (Ge detector).

[c] Analyses obtained using inductively coupled plasma mass spectrometry (ICP-MS). All errors were obtained with calibration standards.

[d] Includes cosmic doses and attenuation with depth calculated using the methods of Prescott and Hutton (1994). Cosmic doses varied from 0.16 to 0.18 Gy/ka.

e Number of replicated equivalent dose (De) estimates used to calculate the equivalent dose. Figures in parentheses indicate total number of measurements included in calculating the represented equivalent dose and age using the minimum age model (MAM). Single grain and single aliquot readings are combined.

f Defined as "over-dispersion" of the De values. Obtained by the "R" factor program. Values >35% are considered to be poorly bleached or mixed sediment.

g Dose rate and age for fine-grained 250-180 microns quartz. Exponential + linear fit used on equivalent dose, errors to one sigma. Datum year assumed to be AD 2010. OSL ages determined by U.S. Geological Survey, Denver, CO.

Table 4. Results of optically-stimulated luminescence ages on quartz grains from soils buried by sand blows (4/30/2020).

Sample Lab No. Depth (m)	Aliquots[a]	Grain Size (µm)	Equivalent Dose (De) (Gy)[b]	Over-dispersion (%)[c]	U (ppm)[d]	Th (ppm)[d]	K (%)[d]	H20 (%)	Cosmic Dose Rate (mGray/yr)[e]	Dose Rate (mGray/yr)	OSL Age (Yr)[f]	OSL Age Yr. B.P. (AD 1950)	Sample Description
SITE DBNW3													
NTR-OSL1 BG4884 0.7	40/40	38-63	12.84 ± 0.5	9 ± 1	2.61 ± 0.01	7.00 ± 0.01	1.86 ± 0.01	10 ± 2	0.18 ± 0.02	2.69 ± 0.06	4,770 ± 215	4,710 ± 215	Buried silty soil collected 3-5 cm below sand blow
NTR-OSL3 BG4885 1.1	39/40	38-63	41.39 ± 1.29	13 ± 1	2.85 ± 0.01	9.10 ± 0.01	1.63 ± 0.01	10 ± 2	0.17 ± 0.02	2.69 ± 0.07	13,370 ± 540	13,310 ± 540	Clayey silty subsoil collected 33-38 cm below sand blow
STR-OSL1 BG4886 1.3	40/40	38-63	39.73 ± 0.95	9 ± 1	3.33 ± 0.01	10.55 ± 0.01	1.63 ± 0.01	10 ± 2	0.17 ± 0.02	3.16 ± 0.07	12,560 ± 405	12,500 ± 405	Clayey silty subsoil collected 32-37 cm below sand blow
SITE DBNW5													
OSL1 BG4894 0.53	20/20	250-355	38.89 ± 1.14	11 ± 2	2.17 ± 0.01	5.87 ± 0.01	1.74 ± 0.01	20 ± 3	0.21 ± 0.02	3.15 ± 0.03	13,950 ± 1,330	12,890 ± 1,330	Buried silty soil collected 3-5 cm below sand blow
OSL2 BG4895 0.77	20/20	150-250	45.28 ± 1.67	15 ± 3	3.20 ± 0.01	8.62 ± 0.01	1.68 ± 0.01	20 ± 3	0.19 ± 0.02	3.41 ± 0.08	17,080 ± 635	17,020 ± 635	Silty subsoil collected 25-30 cm below sand blow

a Aliquots measured and used to define De population by Central Age or Minimum Age Model (Galbraith and Roberts, 2012).

b Equivalent dose calculated on a pure quartz fraction with ultra-small aliquots with 20-80 grains/aliquot and analyzed under blue-light excitation (470 ± 20 nm) by Single Aliquot Regeneration protocols (SAR; Murray & Wintle, 2003; Wintle & Murray, 2006). Equivalent dose (De) was calculated by Central Age or Minimum Age model when overdispersion values are < 20% (at two sigma) and >20% (at two sigma) and assuming a normal data distribution (Galbraith and Roberts, 2012; Liang and Forman, 2019).

c Overdispersion values reflects precision beyond instrumental errors; values of ≤ 20% (at 1 sigma limit) indicate low dispersion in equivalent dose values and defines a unimodal distribution. Values > 20% are associated with mixed equivalent dose signature reflecting multiple grain populations or partial solar resetting.

d U, Th, and K content analyzed by inductively coupled plasma-mass spectrometry by ALS Laboratories, Reno, NV; and includes dose contribution from Rb.

e Includes a cosmic dose rate calculated from parameters in Prescott and Hutton (1994) and includes soft components (Liang and Forman, 2019).

f Systematic and random errors calculated in a quadrature at one standard deviation by the Luminescence Dating and Age Calculator (LDAC) at https://www.baylor.edu/geosciences/index.php?id=962356 (Liang and Forman, 2019). Datum year is AD 2010. OSL ages determined at Geoluminescence Dating Research Laboratory, Dept. of Geosciences, Baylor University, Waco, TX, USA.

Table 5. Results of optically-stimulated luminescence ages on quartz grains from sediment associated with sand blows (4/30/2020).

Sample Lab No. Depth (m)	Aliquots[a]	Grain Size (µm)	Equivalent Dose (De) (Gy)[b]	Over-dispersion (%)[c]	U (ppm)[d]	Th (ppm)[d]	K (%)[d]	Rb (ppm)	H20 (%)	Cosmic Dose Rate (mGray/yr)[e]	Dose Rate (mGray/yr)	OSL Age (Yr)[f]	OSL Age Yr. B.P. (AD 1950)	Sample Description
SITE DBNW5														
OSL3 BG5807 1.65	25/25	32-63	16.27 ± 0.16	6 ± 1	3.53 ± 0.01	10.45 ± 0.01	2.11 ± 0.01	110.0 ± 0.1	15 ± 2	0.175 ± 0.017	3.14 ± 0.06	5,170 ± 120	5,110 ± 120	Top of soil buried by sand blow
OSL4 BG5808 1.78	20/20	32-63	22.74 ± 0.28	5 ± 1	3.44 ± 0.01	10.70 ± 0.01	2.09 ± 0.01	103.5 ± 0.1	15 ± 2	0.172 ± 0.017	3.12 ± 0.06	7,535 ± 235	7,475 ± 235	Clayey silt, 13 cm below OSL3
SITE DBNW7														
OSL1 BG5803 0.46	50/50	250-355	31.98 ± 2.70	44 ± 4	1.26 ± 0.01	4.31 ± 0.01	1.72 ± 0.01	55.5 ± 0.1	10 ± 2	0.220 ± 0.022	1.96 ± 0.05	16,345 ± 1,395	16,285 ± 1,395	Upper portion of sand blow
OSL2 BG5804 1.56	30/32	150-250	120.98 ± 5.44	24 ± 3	3.21 ± 0.01	8.94 ± 0.01	2.06 ± 0.01	79.2 ± 0.1	10 ± 2	0.177 ± 0.018	2.91 ± 0.06	41,505 ± 2,060	41,445 ± 2,060	Top of soil buried by sand blow
OSL3 BG5805 1.68	20/20	32-63	22.74 ± 0.28	5 ± 1	3.21 ± 0.01	9.18 ± 0.01	2.14 ± 0.01	84.2 ± 0.1	10 ± 2	0.174 ± 0.017	3.01 ± 0.06	7,260 ± 180	7,200 ± 180	Clayey silt, 12 cm below OSL2
OSL4 BG5806 0.45	29/30	150-250	35.26 ± 0.21	4 ± 1	1.26 ± 0.01	4.09 ± 0.01	1.78 ± 0.01	56.3 ± 0.1	10 ± 2	0.221 ± 0.022	2.04 ± 0.05	17,265 ± 1,350	17,205 ± 1,350	Upper portion of sand blow
SITE DBNW8														
OSL1 BG5797 0.42	20/20	150-250	39.63 ± 0.46	40 ± 8	1.52 ± 0.01	4.67 ± 0.01	1.80 ± 0.01	59.0 ± 0.1	10 ± 2	0.223 ± 0.022	2.15 ± 0.05	18,435 ± 495	18,375 ± 495	Upper portion of sand blow
OSL2 BG5798 0.92	21/25	150-250	>130	NC	2.23 ± 0.01	5.99 ± 0.01	1.88 ± 0.01	61.2 ± 0.1	10 ± 2	0.1986 ± 0.019	2.4 ± 0.05	>54,200	>54,140	Top of soil buried by sand blow
OSL3 BG5799 1.10	20/20	32-63	59.32 ± 0.79	5 ± 1	3.30 ± 0.01	10.60 ± 0.01	2.12 ± 0.01	92.2 ± 0.1	10 ± 2	0.186 ± 0.019	3.27 ± 0.07	18,115 ± 455	18,055 ± 455	Clayey silt, 18 cm below OSL2
OSL4 BG5800 0.34	24/24	150-250	40.75 ± 2.87	38 ± 6	1.54 ± 0.01	4.81 ± 0.01	1.82 ± 0.01	56.2 ± 0.1	10 ± 2	0.229 ± 0.023	2.18 ± 0.05	18,665 ± 1,345	18,605 ± 1,345	Upper portion of sand blow
OSL5 BG5801 0.95	20/20	32-63	20.12 ± 0.21	4 ± 1	3.57 ± 0.01	9.35 ± 0.01	1.98 ± 0.01	81.9 ± 0.1	10 ± 2	0.185 ± 0.018	3.14 ± 0.07	6,395 ± 150	6,335 ± 150	Buried soil, 8 cm below sand blow

OSL6 BG5802 1.25	23/23	32-63	21.88 ± 1.60	4 ± 1	3.44 ± 0.01	11.20 ± 0.01	1.96 ± 0.01	85.6 ± 0.1	10 ± 2	0.183 ± 0.018	3.18 ± 0.07	15,045 ± 365	14,985 ± 365	Clayey silt, 30 cm below OSL5

[a] Aliquots measured and used to define De population by Central Age or Minimum Age Model (Galbraith and Roberts, 2012).

[b] Equivalent dose calculated on a pure quartz fraction with ultra-small aliquots with 20-80 grains/aliquot and analyzed under blue-light excitation (470 ± 20 nm) by Single Aliquot Regeneration protocols (SAR; Murray & Wintle, 2003; Wintle & Murray, 2006). Equivalent dose (De) was calculated by Central Age or Minimum Age model when overdispersion values are < 20% (at two sigma) and >20% (at two sigma) and assuming a normal data distribution (Galbraith and Roberts, 2012; Liang and Forman, 2019).

[c] Overdispersion values reflects precision beyond instrumental errors; values of ≤ 20% (at 1 sigma limit) indicate low dispersion in equivalent dose values and defines a unimodal distribution. Values > 20% are associated with mixed equivalent dose signature reflecting multiple grain populations or partial solar resetting.

[d] U, Th, Rb and K content analyzed by inductively coupled plasma-mass spectrometry by ALS Laboratories, Reno, NV.

[e] Includes a cosmic dose rate calculated from parameters in Prescott and Hutton (1994) and includes soft components (Liang and Forman, 2019).

[f] Systematic and random errors calculated in a quadrature at one standard deviation by the Luminescence Dating and Age Calculator (LDAC) at https://www.baylor.edu/geosciences/index.php?id=962356 (Liang and Forman, 2019). Datum year is AD 2010. OSL ages determined at Geoluminescence Dating Research Laboratory, Dept. of Geosciences, Baylor University, Waco, TX, USA.

Discussion

The investigations at liquefaction sites – DBNW5, DBNW7, and DBNW8 – located towards the northern end of the DBL, add confidence in the occurrence of a large paleoearthquake ca. 5.4 ka and reduce the uncertainty, or error range, in the estimated timing of the event. The review of previously investigated liquefaction sites – DBSE2, DBNW2, and DBNW3 – has led to revisions in the estimated timing and reduction in the uncertainty of other paleoearthquakes ca. 4.7 ka, 9.8 ka, and 15 ka and 24.3 ka.

^{14}C dating of plant material in the upper few centimeters of soil buried by a sand blow is the best-case scenario for establishing a close maximum constraining age for the sand blow, and thus, the causative earthquake. However, plant material more than 5-10 ka is rarely preserved in buried soils in the Marianna area, especially buried soils within 0.5-1.0 m of the ground surface. If no plant material can be found, thin slices of the upper most 0.25-0.5 centimeter of the buried soil can be collected to date residual carbon in the soil. Residual carbon would have accumulated over a period of time, perhaps 10s-100s of years. Therefore, a soil sample can provide a fairly close maximum constraining age for a sand blow, but probably not as close an age as plant material buried immediately below the sand blow.

OSL dating of a buried soil also can provide fairly close maximum constraining ages for sand blows. However, for OSL dating to provide a meaningful age estimate of the time of burial by the sand blow, the luminescence in the quartz grain being dated had to be completely reset by exposure to the sun. Another potential problem is post-event bioturbation of the buried soil by tree roots can mix the soil both with vented sand above and subsoil below, possibly leading to dating of grains that had been exposed to the sun some time prior to the event. In the Marianna sand blows, bioturbation by roots often extends to 1.0-1.5 m below the ground surface. Therefore, samples collected below the zone of bioturbation are more likely to provide meaningful results.

Dispersion, also known as scatter, measured during the OSL dating process reflects the degree of solar resetting or mixing of grain populations (Forman et al., 2000; Galbraith and Roberts, 2012; Liang and Forman, 2019). For a sample collected from the buried soil, an OSL age with low dispersion is more likely to reflect the time of burial by the sand blow; whereas, an OSL age with a high dispersion value is likely to be older than the time of burial due either to partial solar resetting or to bioturbation. OSL samples collected from the sand blows had high dispersion values suggesting that they were mixed and/or partially bleached. We surmise that rapid deposition of the slurry of water and entrained sediment vented to the surface as a result of liquefaction prohibited complete solar resetting of luminescence in the sand grains. Therefore, OSL ages of the sand blows are likely to be older than the time of formation of the sand blows.

The chronology of paleoearthquakes in the Marianna area is likely to be complete for the Holocene, but incomplete for the Late Pleistocene. There are many more sand blows in the area that could be studied in order to better understand the Late Pleistocene earthquake history in the Marianna area. Identification of Late Pleistocene sand blows to study is challenging but critical. Degree of weathering of sand blows is a useful indicator of advanced age. We have found that the older sand blows and related dikes have deep weathering profiles, substantial development of soil lamellae, and accumulation of fines especially above buried soils. However, to recognize these characteristics, the sand blows must be trenched. Remote sensing may be a useful tool to identify older extremely weathered sand blows prior to trenching. This potential tool is currently being tested in the Marianna area.

A better understanding of the paleoearthquake history of the Marianna area would improve our understanding of the recurrence times of large-magnitude earthquakes and the long-term behavior of the Marianna source. In addition, the Marianna paleoearthquake history combined with that of other areas, such as the New Madrid seismic zone, would provide insights regarding spatial and temporal migration of seismicity across the region which would have significant implications for earthquake hazard assessment in the central United States. In the Marianna area and across the Mississippi River Valley, however, sand blows are being destroyed by land grading and mining for agricultural and construction purposes, respectively. Therefore, time is of the essence for recovering the record of paleoearthquakes in the region before it is lost forever.

Conclusions

The main findings of this project are as follows:

- The Marianna chronology of paleoearthquakes is revised to ca. 4.7 ka, 5.4 ka, 6.8, 9.8 ka, 15 ka, and 24.3 ka;
- The uncertainty in estimated timing of Holocene paleoearthquakes is about ± 100 yr; whereas, the uncertainty in estimated timing of Late Pleistocene events is about ± 2-4 kyr;
- Dating older sand blows, especially those more than 10 kyr old, is very challenging due to weathering processes and bioturbation;
- Pre-event surface soils buried by sand blows more than 1.5 m thick offer the best opportunity to collect samples for ^{14}C and OSL dating that will provide close or fairly close maximum constraining ages for the formation of the sand blow and thus the timing of the causative earthquake;
- The Marianna chronology of paleoearthquakes is likely to be complete for the Holocene, but not for the Pleistocene;
- Additional study of Late Pleistocene sand blows in the Marianna area is needed to better understand the recurrence times of large-magnitude earthquakes in the area, the long-term behavior of the Marianna source, and the spatial and temporal migration of seismicity across the central United States.

Acknowledgments

Beta Analytic, Inc. performed radiocarbon dating of organic samples and Steve Forman of Geoluminescense Dating Research Laboratory at Baylor University preformed the OSL dating of sediment samples. Martha Kopper of the Arkansas Geological Survey assisted with paleoseismological field work and facilitated excavation of trenches. Kathy Tucker updated the regional paleoliquefaction database as well as maps of the Marianna area and surrounding region showing liquefaction sites, mapped faults, and topography. Thanks to the property owners and farmers who gave us permission to carry out field work at the study sites southwest of Marianna, Arkansas. The material presented in this report is based upon work supported by the U.S. Geological Survey under Grant No. G22AP00335.

References Cited

Bronk Ramsey, C., 2008, Bayesian analysis of radiocarbon dates, Radiocarbon, v. 51, n. 1, p. 337-360.

Chlaib, H. K., Mahdi, H., Al-Shukri, H. J., Su, M., Catakli, A., and Abd, N., 2014, Using ground penetrating radar to detect small-scale animal burrows, Journal of Applied Geophysics, doi: https://doi.org/10.1016/j.jappgeo.2014.01.011.

Forman, S. L., Pierson, J., and Lepper, K., 2000, Luminescence Geochronology, Quaternary Geochronology: Methods and Applications: AGU Reference Shelf 4, p. 157-175.

Hildenbrand, T. G., and Hendricks, J. D., 1995, Geophysical setting of the Reelfoot Rift and relations between rift structures and the New Madrid seismic zone, U.S. Geological Survey, Professional Paper 1538-E.

Hough, S. E., 2004, Scientific overview and historical context of the 1811-1812 New Madrid earthquake sequence, Annals of Geophysics, v. 47, n. 2/3, p. 523-537.

Hussein, R., Hanan M., and Al-Shukri, H., 2023, Integrating GPR with ArcGIS Pro to map the Central Arkansas water pipelines beneath the old Broadway Bridge, Little Rock, Journal of Applied Geophysics, v. 215, 18p.

Juang, C. H., and Jiang, T., 2000, Assessing probablistic methods for liquefaction potential evaluation, Soil Dynamics and Liquefaction 2000, GSP 107 (Proceedings GeoDenver), American Society of Civil Engineers, Reston, VA.

Juang, C. H., Zhang, J., Khoshnevisan, S., and Gong, W., 2017, Probabilistic methods for assessing soil liquefaction and effect, Geo-Risk 2017: Keynote Lectures, American Society of Civil Engineers, p. 122-145, https://doi.org/10.1061/9780784480694.

Liang, P., and Forman, S. L., 2019, LDAC: An Excel-based program for luminescence equivalent dose and burial age calculations, Ancient TL, v. 37, p. 21-40.

Murray, A. S. and Wintle, A. G., 2003, The single aliquot regenerative dose protocol: potential for improvements in reliability, Radiation Measurements, v. 37, p. 377–381.

Obermeier, S. F., 1989, The New Madrid earthquakes: an engineering-geologic interpretation of relict liquefaction features, U.S. Geological Survey, Professional Paper 1336-B.

Obermeier, S. F., 1996, Using liquefaction-induced features for paleoseismic analysis, *in* McCalpin, J. P., ed., Paleoseismology, Academic Press, San Diego, CA, p. 331-396.

Odum, J. K., Williams, R. A., Stephenson, W. J., Tuttle, M. P., Al-Shukri, H., 2016, Preliminary assessment of a previously unknown fault zone beneath the Daytona Beach sand blow cluster near Marianna, Arkansas, Seismological Research Letters, v. 87, n. 6, p. 1453-1464.

Petersen, M. D., et al., 2014, Documentation for the 2014 Update of the United States National Seismic Hazard Maps, U.S. Geological Survey Open-File Report 2014–1091, 243 p.

Petersen, M. D., Shumway, A. M., Powers, P. M., Field, E. H., Moschetti, M., Jaiswal, K. S., Milner, K. R., Rezaeian, S., Frankel, A. D., Llenos, A. L., et al., 2024, The 2023 U.S. 50-State National Seismic Hazard Model: Overview and implications, Earthquake Spectra, v. 40, n. 1, p. 5-88, doi: https://doi.org/10.1177/87552930231215428.

Prescott, J. R., and Hutton, J. T., 1994, Cosmic ray contributions to dose rates for luminescence and ESR dating: Large depths and long-term time variations, Radiation Measurements, v. 23, p. 497-500.

Al-Qadhi, O, 2010, Geophysical investigation of paleoseismological features in eastern Arkansas, USA: Ph.D dissertation, University of Arkansas at Little Rock, Little Rock, Arkansas, 235 p., plus Appendix A.

Rains, D. S., and Guccione, M. J., 2016, Formation of the Marianna Gap, a transverse stream valley, through Crowley's Ridge, northern Mississippi alluvial valley, U.S.A., Seismological Research Letters, v. 87, n. 6, p. 1442-1452.
Reimer, P. J., Austin, W. E. N., Bard, E., Bayliss, A., Blackwell, P. G., Bronk Ramsey, C., Butzin, M., Cheng, H., Edwards, R. L., Frederick, M., et al., 2020, The IntCal20 northern hemisphere radiocarbon age calibration curve (0-55 cal kBP), Radiocarbon, v. 62, n. 4, p. 725-757. doi: 10.1017/RDC.2020.41
Robertson, P. K., 2010, Evaluation of flow liquefaction and liquefied strength using the CPT, Journal of Geotechnical and Geoenvironmental Engineering, v. 136, n. 6, p. 842-853.
Saucier, R. T., 1977, Effects of the New Madrid earthquake series in the Mississippi alluvial valley, U.S. Army Corps of Engineers Waterways Experiment Station Miscellaneous Paper S-77-5*,* 10.
Schumm, S. A., and Spitz, W. J., 1996, Geological influences on the lower Mississippi River and its alluvial valley: Engineering Geology, v. 45, pp. 245-261.
Seed, H. B. and Idriss, I. M., 1971, Simplified procedure for evaluating soil liquefaction potential, Journal of the Soil Mechanics & Foundations Division (ASCE), v. 97 (SM9), p. 1249-1273.
Seed, H. B., and Idriss, I. M., 1982, Ground motions and soil liquefaction during earthquakes, Earthquake Engineering Research Institute, Berkley, 134 p.
Al-Shukri H. J., Lemmer, R. E., Mahdi, H. H., and Connelly, J. B., 2005, Spatial and temporal characteristics of paleoseismic features in the southern terminus of the New Madrid seismic zone in eastern Arkansas, Seismological Research Letters, v. 76, p. 502-511.
Al-Shukri, H., Mahdi, H., and Tuttle, M., 2006, Three-dimensional imaging of earthquake-induced features with ground penetrating radar, near Marianna, Arkansas, Seismological Research Letters, v. 77, p. 505-513.
Al-Shukri, H., Mahdi, H., Al-Qadhi, O., and Tuttle, M. P., 2009, Spatial and temporal characteristics of paleoseismic features in the southern terminus of the New Madrid seismic zone in eastern Arkansas, Final Technical Report, Prepared for U.S. Geological Survey award 1434-07HQGR0069, 24 p.
Al-Shukri, H., Mahdi, H., Tuttle, M. P., Dyer-Williams, K., 2015, Geophysical and paleoseismic investigations of large sand blows along a northwest-oriented lineament near Marianna, Arkansas, Final Technical Report, Prepared for U.S. Geological Survey award G12AP20093, 31 p.
Technical Report, 2012, The Central and Eastern U.S. seismic source characterization for nuclear facilities, U.S. Nuclear Regulatory Commission and Electric Power Research Institute, Palo Alto, CA.
Thompson Jobe, J. A., Hatem, A. E., Gold, R. D., DuRoss, C. B., et al., 2022, Revised earthquake geology inputs for the central and eastern United States and southeast Canada for the 2023 U.S. 50-State National Seismic Hazard Model, Seismological Research Letters, v. 93, n. 6, p. 3100-3120, doi: https://doi.org/10.1785/0220220162.
Tuttle, M. P., 2001, The use of liquefaction features in paleoseismology: Lessons learned in the New Madrid seismic zone, central United States, Journal of Seismology, v. *5*, p. 361-380.
Tuttle, M. P., Al-Shukri, H, and Mahdi, H., 2006, Very large earthquakes centered southwest of the New Madrid seismic zone 5,000-7,000 years ago, Seismological Research Letters, v. 77, n. 6, p. 664-678.

Tuttle, M. P., and Hartleb, R., 2012, Appendix E. Central and eastern U.S. paleoliquefaction database, uncertainties associated with paleoliquefaction data, and guidance for seismic source characterization, *in* The Central and Eastern U.S. Seismic Source Characterization for Nuclear Facilities, Technical Report, EPRI, Palo Alto, CA, U.S. DOE, and U.S. NRC, 135 p., plus database.

Tuttle, M. P., Hartleb, R., Wolf, L., and Mayne, P. W., 2019a, Paleoliquefaction studies and the evaluation of seismic hazard, Geosciences, v. 9, n. 7, 61 p, doi:10.3390/geosciences9070311.

Tuttle, M. P., Wolf, L. W., Dyer-Williams, K., Mayne, P. W., and Lafferty, R. H., et al., 2019b, Paleoliquefaction studies in moderate seismicity regions with a history of large earthquakes, U.S. Nuclear Regulatory Agency, NUREG/CR-7257, 450 p.

Tuttle M. P., Al-Shukri, H, and Mahdi, H., 2020, Geophysical and paleoseismic investigations of large sand blows along a northwest-oriented lineament near Marianna, Arkansas, Final Technical Report, U.S. Geological Survey award G18AP00083, 31 p.

Van Arsdale, R., and Cupples, W., 2013, Late Pliocene and Quaternary deformation of the Reelfoot Rift, Geosphere, v. 9, no. 6., p. 1819-1831.

Wheeler, R. L., Omdahl, E. M., Dart, R. L., Wilkerson, G. D., and Bradford, R. H., 2003, Earthquakes in the central U.S., 1699-2002, U. S. Geological Survey, Geological investigations series I-2812.

Wintle, A. G. and Murray, A. S., 2006, A review of quartz optically stimu- lated luminescence characteristics and their relevance in single-aliquot regeneration dating protocols, Radiation Measurements, v. 41, p. 369–391.

Youd, T. L., et al., 2001, Liquefaction resistance of soils: Summary report from the 1996 NCEER and 1998 NCEER/NSF workshops on evaluation of liquefaction resistence of soils, Journal of Geotechnical and Geoenvironmental Engineering, v. 127, n. 10, p. 817-833.

Youd, T. L., and Idriss, I. M., 2003, Liquefaction resistance of soils: Summary report from the 1996 NCEER and 1998 NCEER/NSF workshops on evaluation of liquefaction resistance of soils: Closure and Errata, Journal of Geotechnical and Geoenvironmental Engineering, v. 129, n. 3, 285 p.

Project Data

Data is made available to the public is this report, a paper in preparation to be submitted for publication in a peer-reviewed journal. In addition, information about liquefaction sites, liquefaction features, and results of dating have been entered into a database that is available to the public for download as both Excel files and Shapefiles from https://mptuttle.com/databases.html.

Bibliography of Related Publications

Al-Qadhi, O, 2010, Geophysical investigation of paleoseismological features in eastern Arkansas, USA: Ph.D dissertation, University of Arkansas at Little Rock, Little Rock, Arkansas, 235 p., plus Appendix A.

Al-Shukri H. J., Lemmer, R. E., Mahdi, H. H., and Connelly, J. B., 2005, Spatial and temporal characteristics of paleoseismic features in the southern terminus of the New Madrid seismic zone in eastern Arkansas, Seismological Research Letters, v. 76, p. 502-511.

Al-Shukri, H., Mahdi, H., and Tuttle, M., 2006, Three-dimensional imaging of earthquake-induced features with ground penetrating radar, near Marianna, Arkansas, Seismological Research Letters, v. 77, p. 505-513.

Al-Shukri, H., Mahdi, H., Al-Qadhi, O., and Tuttle, M. P., 2009, Spatial and temporal characteristics of paleoseismic features in the southern terminus of the New Madrid seismic zone in eastern Arkansas, Final Technical Report, Prepared for U.S. Geological Survey award 1434-07HQGR0069, 24 p.

Al-Shukri, H., Mahdi, H., Tuttle, M. P., Dyer-Williams, K., 2015, Geophysical and paleoseismic investigations of large sand blows along a northwest-oriented lineament near Marianna, Arkansas, Final Technical Report, Prepared for U.S. Geological Survey award G12AP20093, 31 p.

Tuttle, M. P., Al-Shukri, H, and Mahdi, H., 2006, Very large earthquakes centered southwest of the New Madrid seismic zone 5,000-7,000 years ago, Seismological Research Letters, v. 77, n. 6, p. 664-678.

Tuttle, M. P., and Hartleb, R., 2012, Central and eastern U.S. paleoliquefaction database, uncertainties associated with paleoliquefaction data, and guidance for seismic source characterization, Appendix E. *in* The Central and Eastern U.S. Seismic Source Characterization for Nuclear Facilities, Technical Report, EPRI, Palo Alto, CA, U.S. DOE, and U.S. NRC, 135 p. plus database.

Tuttle M. P., Al-Shukri, H, and Mahdi, H., 2020, Geophysical and paleoseismic investigations of large sand blows along a northwest-oriented lineament near Marianna, Arkansas, Final Technical Report, U.S. Geological Survey award G18AP00083, 31 p.

Tuttle, M. P., Al-Shukri, H, Mahdi, H., Ameen, T., Hussein, R., Forman, S. L., Dyer-Williams, K., Hopper, M., and Tucker, K., 2025, Repeated large magnitude earthquakes during Middle-Early Holocene and Late Pleistocene in the Marianna area of Arkansas, to be submitted to Seismological Research Letters, *in prep*.